Rigid Pavement: Ontario Calibration of the Mechanistic-Empirical Pavement Design Guide Prediction models

by

Jian Zhong

A thesis

presented to the University of Waterloo

in fulfillment of the

thesis requirement for the degree of

Master of Applied Science

in

Civil Engineering

Waterloo, Ontario, Canada, 2017

AUTHOR'S DECLARATION

I hereby declare that I am the sole author of this thesis. This is a true copy of the thesis, including any required final revisions, as accepted by my examiners.

I understand that my thesis may be made electronically available to the public.

ABSTRACT

The Mechanistic-Empirical Pavement Design Guide (MEPDG) has been introduced to transportation agencies as an innovative method for analysis and design of pavements. However, the MEPDG cannot be used by highway agencies without calibration due to the different situations in Canada. Local calibration the MEPDG, which means adjusting the coefficients of performance prediction models to meet the local conditions, should be an essential step for any agencies before the official acceptation of the MEPDG.

As the part of the project, Local Calibration of the MEPDG Prediction Models Using More Accurate Field Measurements funded by Highway Infrastructure Innovation Funding Program (HIIFP), this research involved the local calibration of the models for Jointed Plain Concrete Pavement (JPCP) in the Province of Ontario. Using the field measurements collected by Ministry of Transportation in Ontario (MTO), the study performed local calibration for 32 rigid (JPCP) pavement sections. The primary objective of this study was to examine prediction results using global models; then if not agree with the measurements, refine the coefficients of the MEPDG performance models using the nonlinear optimization methods. The proposed calibration was applied by using the sections located in different zones throughout Ontario to represent the local features, including climate and traffic conditions. Finally, the local calibration results are presented and compared with previous results of global models to assess the robustness of local calibration. The research shows the feasibility of the mathematical optimization method for in local calibration in Ontario, and it also provides some useful findings for future uses of the MEPDG.

ACKNOWLEDGMENTS

First of all, I would like to thank my supervisor, Professor Susan Tighe, for her kind support in this study. I especially admire her great technical knowledge, academic reputation and ability to manage people.

Furthermore, I would like to acknowledge my colleagues in CPATT, Ph.D. Candidate Daniel Pickel and Ph.D. Candidate Shi Dong, for their constructive comments and advice throughout the course of this research.

Also, special thanks are extended to Drs. Li Ningyuan and Mr. Warren Lee for their passionate and invaluable assistance to my research. Mr. Lee gave me a lot suggestion on the thesis, and Dr. NinYuan Li provided me with the manual of MTO's pavement management system. We are also grateful for the funding for the project under the Ministry of Transportation Ontario Highway Infrastructure Innovation Funding Program (HIIFP).

I also would like to acknowledge the MTO and the engineers of ARA, Inc., who helped me to overcome some difficulties in my study. I would be grateful for the help of my friends, the department faculty and staff at University of Waterloo.

Last but not the least, I would like to thank my family for supporting me throughout writing this thesis and my life in general.

TABLE OF CONTENTS

LIST OF TABLES

LIST OF FIGURES

CHAPTER 1 INTRODUCTION

1.1 Background

The pavement design method from the *Guide for the Design of Pavement Structures* (AASHTO 1993) is based on the empirical performance equations obtained from the AASHTO Road test and is still used in many countries around the world. This method can only be applied to given materials, traffic loading, and environmental condition. To overcome this limitation, the United States National Cooperative Highway Research Program (NCHRP) proposed Project 1-37 on Development of a 2002 guide for the design of new and rehabilitated pavement structures. Subsequently, in March 2004, the *Guide for Mechanistic-Empirical Design of New and Rehabilitated Pavement Structures* was released under the NCHRP Project 1-37A (NCHRP 2004). At the same time, the initial Mechanistic-Empirical Pavement Design Guide (MEPDG) Software was developed by Applied Research Associates Inc. (ARA Inc. 2004). To improve the accuracy of prediction models for application, several national-level research programs, funded by the NCHRP Project 1-40 (NCHRP 2006a, NCHRP. 2006b, NCHRP. 2007) and Federal Highway Administration (FHWA), were conducted on the procedure for the local calibration of the MEPDG (FHWA 2010a, FHWA 2010b). It should be noted that the *Guide for the Local Calibration of the Mechanistic-Empirical Pavement Design Guide* (AASHTO 2010) was a milestone for the calibration, which summarized the exact procedures in the local calibration systematically. The MEPDG Software was then developed under the name of AASHTOWare Pavement ME Design software (AASHTOWare®) in February 2013. The latest AASHTOWare® is version 2.3.1, which was released in August 2016.

In Canada, the MEPDG is currently being adopted since the implementation of NCHRP 1-37A and 1-40 Projects (AASHTO 2010). Although this development was led by the America Association of State Highway and Transportation Organization (AASHTO), many Canadian agencies were involved in the development and had also wanted to implement this pavement design tool. The MEPDG provides an innovative pavement analysis and design tool by utilizing mechanical method to calculate pavement responses (stresses, strains, and deflections) and empirical models to predict pavement performance.

The development of the Guide for Design of New and Rehabilitated Pavement Structures (AASHTO 2002) started in 1996, and the primary objective was to develop a mechanistic-empirical (ME) design method that combined mechanistic models and the databases relevant to the pavement performance prediction.

The MEPDG involves computing incremental distress predictions over time by using pavement responses (stresses, strains, and deflections) generated from a mechanistic module with the inputs of traffic loading, material properties, and environmental data. The output of the MEPDG is predictions of distresses and smoothness with reliability values. In the application of the MEPDG, the design is an iterative process based on the results of trial plans proposed by the designer. If the predictions cannot meet the performance criteria at the given reliability provided by local agencies, the design is revised, and the procedure is repeated.

When the MEPDG was being proposed, the NCHRP (2004) recommended that state and provincial departments of transportation (DOTs) conduct local calibration of the MEPDG models before fully implementing the software (Kaya 2013). This is because that the variety of local climate, material properties, traffic conditions, and maintenance activities may have impacts on the prediction results using the MEPDG. Also, AASHTO (2010) states that "policies on pavement preservation and maintenance, construction and material specifications, and materials vary across the country and are not considered directly in the MEDPG" and recommends employing local calibration studies to take these regional differences into account (Ceylan and Gopalakrishnan 2007). Although the calibration guide (AASHTO 2010) provides a stepwise procedure, the exact approach still needs to be developed in terms of the actual situation.

The local calibration involves a mathematical process to minimize the bias and standard error between observed pavement distress values and pavement performance predictions and makes the software output more reliable (AASHTO 2010). Such local-calibration studies are needed for all agencies when the performance model predictions do not agree with the measurements. The Ministry of Transportation of Ontario (MTO) has decided to adopt the MEPDG as a possible future pavement design tool; therefore, it is urgent to calibrate the coefficients in the transfer functions in the MEPDG to make the predictions correct and reliable under the conditions in Ontario.

The Long Term Pavement Performance (LTPP) program received its foundational mission in 1984, which was "increase pavement life by the investigation of the long-term performance of various designs of pavement structures and rehabilitated pavement structures, using different materials and under different loads, environments, subgrades, soils, and maintenance practices." The plan proposed a 20-year study on in-service pavements across the United States. Globally-calibrated performance models were mostly based on the data from the Long-Term Pavement Performance (LTPP) test sections. Due to the uneven distribution of testing sites, the conditions in some regions cannot be represented in the global calibration models. However, the local calibration can result in the MEPDG providing pavement design and performance conditions that reflect the local conditions, including materials and local policies.

Although the MEPDG Local Calibration Guide (AASHTO 2010) provides a step-by-step methodology, the existing local calibration studies have not discussed their optimization procedures in detail and a detailed procedure of local calibration in Ontario is needed. The selection of testing roads and particular optimization step are identified in this procedure. Once this process is finalized, it is expected to be used by local highway engineers and their counterparts in Ontario, and provides a cost effective design and an accurate prediction of performance for MTO in terms of the local conditions. With the help of these accurate performance predictions during the pavement service life, engineers will take necessary and timely precautions as needed and determine the right pavement thickness for rehabilitation.

"Great efforts have been invested by the MTO in calibrating the mechanistic-empirical pavement design guide (MEPDG) and the companion software (AASHTOware Pavement ME Design®) to the local condition and practice of pavement design in Ontario"(Yuan

2015). In fact, several MTO projects have been conducted to develop the local calibration over the past few years for flexible pavements. Based on these projects, some achievements of local calibration, including mathematical algorithms of optimization, have been obtained. However, due to the limited amount of LTPP data on the rigid pavement in Ontario, the current local calibration for the rigid pavement had not been conducted until this project was launched.

As the primary objective of local calibration, determination of the coefficients within prediction models is a critical step in this process. The procedure employed in previous studies mainly focused on the trial-and-error approach requiring many MEPDG runs with adjusted calibration coefficients. Kaya pointed that "The main reasons for the use of this approach in previous studies are related to: (1) lack of understanding pavement performance models comprised of numerous equations; (2) neglecting the review of numerous intermediate output files (mostly, text file format) produced along with final result summary output files (PDF and Excel file formats); and (3) pavement response results previously not provided by MEPDG software but now provided by Pavement ME Design software through intermediate output files." (Kaya 2013)

This study focuses on applying the method above to local calibrate the prediction models for the rigid pavements in Ontario, including transverse cracking, faulting, and international roughness index. However, the currently available data for rigid pavement is limited. Thus, various statistical approaches are developed to ensure the results to be acceptable. This research uses data provided by MTO, and the project was funded by the Highway Infrastructure Innovation Funding Program (HIIFP).

1.2 Scope and Objectives

The first objective of this study is to evaluate the accuracy of a globally calibrated pavement performance prediction models by using MTO Pavement Management System (PMS) data. The second objective of this study is to conduct a calibration of these models if their accuracy is not enough to meet the requirements of local conditions, such as local policies, weather, and traffic. This process was executed using MEPDG version 2.1.3, released in

August 2016, with the assistance of a series of techniques including sensitivity analysis, and linear and nonlinear optimization methods for improving model prediction accuracy. The proposed research scope involved the Ontario local calibration of Joint Plain Concrete Pavement (JPCP) using more accurate field measurements and forensic investigations, for JPCP is the most common type of concrete pavement in this province.

1.3 Methodology

The local calibration is a process by adjusting the coefficients of performance models based on the insitu measurements provided by MTO. The main steps are briefly described below:

- Rigid pavements test sections were selected in different regions of Ontario, and a wide range of traffic loads, age, and climatic conditions was taken into account. Pavements constructed after 1989 were assumed to reflect modern construction procedures.
- Local road agencies provided design information of pavement structure, traffic volume, and international roughness index (IRI). Weather data were obtained from the weather station located near to the selected sections. The information was then processed and used as input data for the MEPDG software.
- With the default (global calibration) factors, distress predictions were determined. Afterward, the fitness of predicted values and average observed distress data were assessed for a series of distress models on the rigid pavements (transverse joint faulting, slab cracking, and international roughness index (IRI)).
- Adjustments of the calibration factors were undertaken based on a sensitivity analysis of each coefficient and determined by using several mathematical approaches to minimize the difference between the prediction values and observed values.
- The transfer functions was based on the metric system, however, in the calculation process English system was also employed, in case of the difficulty in the conversion between the two in transfer functions.

Overall, this research follows the basic principle proposed by the AASHTO local calibration guide in 1-40A but also incorporates tools to address the special issues that were encountered to accomplish the local calibration in Ontario. The proposed local calibration methodology was applied to 32 new constructed sections located in different zones throughout Ontario to represent the features of the various regions in Ontario.

1.4 Thesis Organization

This thesis consists of five chapters. Chapter 1 includes the background and objectives of this study. Chapter 2 provides a summary of literature review results related to local calibration of MEPDG. Chapter 3 documents the local calibration methodology used in this study, including the descriptions of Ontario pavement sites selection, calibration databases for Ontario pavement systems, optimization approaches and accuracy evaluation criteria. Chapter 4 presents local calibration results for each pavement type. Chapter 5 provides discussion on future enhancements of Pavement ME Design, conclusions and recommendations, contributions of this study to the literature, and state-of-the-art practices as well as recommendations for future research.

Chapter 2 LITERATURE REVIEW

As the name implies, rigid pavements behave rigidly. They are constructed using cement concrete, aggregate, water, and additives, and flex only slightly under heavy loading. Their load carrying capacity is mainly due to this property. This chapter will mainly focus on the history of rigid of pavement design, the MEPDG method of rigid pavement design, and calibration of the MEPDG.

2.1 History of Rigid Pavement Design

Concrete pavement design is based on the accumulation and summary of knowledge gained through decades of engineering experiences. In Canada the first concrete road was built in 1890 in Toronto, Ontario. Several theoretical methods were developed based on the analytical solutions, which were not initially affected by various factors similar to the development of flexible pavement design. (Huang 2003)

Goldbeck first developed an analytical solution for pavement slab design by treating it as a cantilever beam in 1919. The most extensive studies on stresses, strains, and deflections in the rigid pavement were exploited by Westergaard, who assumed that the active pressure between the slab and the subgrade at any given point is proportional to the deflection of that point, independent of deformation at any other points. As he indicated, this type of foundation is called a liquid or Winkler foundation with every point in full contact. (Huang 2003)

Because of the disagreement with the field observed values and theoretical results based on Winkler foundation, Pickett pointed out the model equation always yielded a small stress value at the corner of the slab. By assuming each part of the slab is not in full contact with the subgrade, Pickett developed his own solutions in terms of experience and experimental results and tried to use the solid model as a simulation. However, the solution for the theoretical model is too complex to employ in most real situations, and a simple method based on solid foundations was developed to determine stresses and deflections. (Huang 2003)

With the advent of modern computers, the numerical method for pavement design was feasible. For example, the assumption of full contact with subgrade in slab solutions is impossible in the traditional method because of the complex calculations in terms of moisture warping, temperature curling, and pumping. But with the help of computers, the numerical methods such as the finite element method can be employed for analyzing slab on elastic subgrades of both liquid and solid types. Subsequently, a series of professional Finite Element software programs were developed, including WESLAYER, WESLIQUID, and ILLI-SLAB. Still, some general-purpose finite element packages, like ABAQUS, were used to analyze pavement in some specific areas, e.g. liquid or solid types. These endeavors have achieved a lot of useful results (Huang 2003).

Beside the theoretical methods mentioned above, the empirical approach is another important method in pavement design with long history. It is based on the results of experiments or experience it requires a number of observations, which are used to ascertain the relationships between the design inputs, including loads, materials, layer configurations, and weather condition, and outcomes, like dimensions of the pavement (Li et al. 2011). For example, in 1984 the Portland Cement Association (PCA) provided a standard procedure which was based on the testing results and data in AASHTO Road Programs, and led the process to design with tables and nomographs developed by PCA.

The AASHTO Design Guide for Rigid Pavement (AASHTO 1993) also provided an empirical method based on a huge amount of data collected from the AASHTO road tests since 1960s. In addition, several additional terms were considered in the procedure of designing, such as reliability and standard deviation, material features. Some changes in rehabilitation design were also involved in this design guide (AASHTO 1993). These improvements, in terms of mechanistic rules and engineering experience, aimed to make the design method satisfy a broad range of conditions other than those of AASHO Road Test.

The design guide was widely used because the empirical approach simply specifies pavement structural designs based on the experience in the past. Although there are some improvements referred to interactions with environment and materials, long term effects on pavements cannot be taken into account with this empirical method.

To update the Guide for Design of Pavement (AASHTO 1993), pavement engineers were trying to find a real integration of these observations over the past decades and to develop a rational pavement design method with mechanistic underpinnings (Waseem 2013).

2.2 The MEPDG Method

The MEPDG combines a mechanistic approach with the empirical method and is applied in both new construction and rehabilitation rigid pavement design. It was first released in 2004 under the NCHRP Project 1-37A, and provided more significant potential benefits than in the 1993 AASHTO Guide. The MEPDG can predict several distress types, such as surface roughness, transverse cracking, and faulting in rigid pavement (TAC 2013). It also offers procedures for evaluating existing pavements and recommendations for rehabilitation treatments, drainage, and foundation improvements.

As the name of Mechanistic–Empirical implies, this method was the combination of mechanical principles with empirical results. The general methodology of the MEPDG can be understood by the schematic in Figure 2-1.

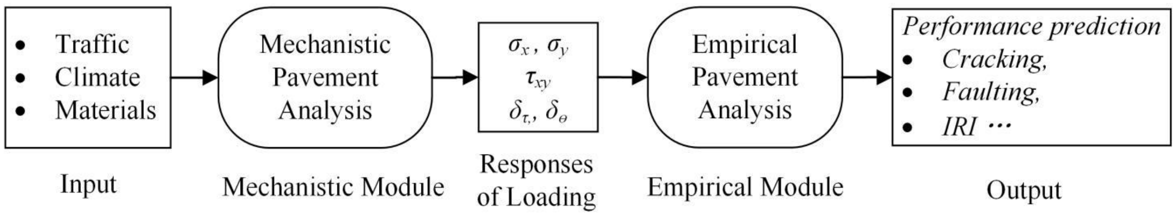

Figure 2-1 Schematic of MEPDG

The MEPDG programs sponsored by AASHTO and NCHRP promoted the implementation of ME method as an effective design method in the DOTs. The research reports from these programs are listed in Table 2-1 to illustrate the progress of implementation.

An independent review of the application of NCHRP project 1-37A was completed in the name of NCHRP project 1-40A (Brown et al. 2006), which involved a number of issues to be solved in the implementation of the guide. These issues were addressed in NCHRP project 1-40D and reported in *Independent Review of the Mechanistic-Empirical Pavement Design Guide and Software* (Barenberg et al. 2006).

Table 2-1 Progress of Implementation of MEPDG

Author	Publication Year	Title	Report/Project Number
NCHRP	2004	*Guide for Mechanistic-Empirical Design of New and Rehabilitated Pavement Structures*	Project 01-37A
NCHRP	2005	*Traffic Data Collection, Analysis, and Forecasting for Mechanistic Pavement Design*	Project 01-39, Report 538
NCHRP	2006	*Independent Review of the Mechanistic-Empirical Pavement Design Guide and Software*	Project 01-40A, Digest 307
NCHRP	2006	*Changes to the Mechanistic-Empirical Pavement Design Guide Software Through Version 0.900*	Project 01-40D, Digest 308
AASHTO	2008	*Mechanistic-Empirical Pavement Design Guide: A Manual of Practice*	AASHTO 2008
NCHRP	2009	*Local Calibration Guidance for the Recommended Guide for Mechanistic-Empirical Pavement Design of New and Rehabilitated Pavement Structures*	Project 01-40B
NCHRP	2010	*Models for Predicting Reflection Cracking of Hot-Mix Asphalt Overlays*	Project 01-41, Report 669
AASHTO	2010	*Guide for the Local Calibration of the Mechanistic-Empirical Pavement Design Guide*	AASHTO 2010
FHWA	2010	*Local calibration of the MEPDG using pavement management*	DTFH61-07-R-00143
NCHRP	2011	*Sensitivity Evaluation of MEPDG Performance Prediction*	Project 1-47
AASHTO	2011	*Software Help System DARWin-ME Mechanistic-Empirical Pavement Design Software*	AASHTO 2011
AASHTO	2013	*AASHTOWare Pavement ME Design User™ Manual*	AASHTO 2013
NCHRP	2013	*Guide for Conducting Forensic Investigations of Highway Pavements*	Project 01-49, Report 474
NCHRP	2014	*Implementation of the AASHTO Mechanistic-Empirical Pavement Design Guide and Software: A Synthesis of Highway Practice*	Project 20-05, Report 457
NCHRP	2015	*Consideration of Preservation in Pavement Design and Analysis Procedures*	Project 01-48, Report 810

The progress of the MEPDG consists of three major stages, shown in Figure2-2. In stage 1, local policies and strategies are identified, along with foundation analysis. In addition, pavement materials, traffic data, and hourly climatic data (temperature, precipitation, solar radiation, cloud cover, and wind speed) from weather stations are developed. In stage 2, a structural/performance analysis is implemented by analyzing sections over time using the pavement response and various distress models to determine the damage over time. A pavement structural design is then obtained through this iterative process in which the prediction performance is compared against the design criteria or policies until all design criteria or policies are satisfied to some specified reliability level. In stage 3, assessments are conducted on viable alternatives, engineering analysis, and life cycle cost analysis.

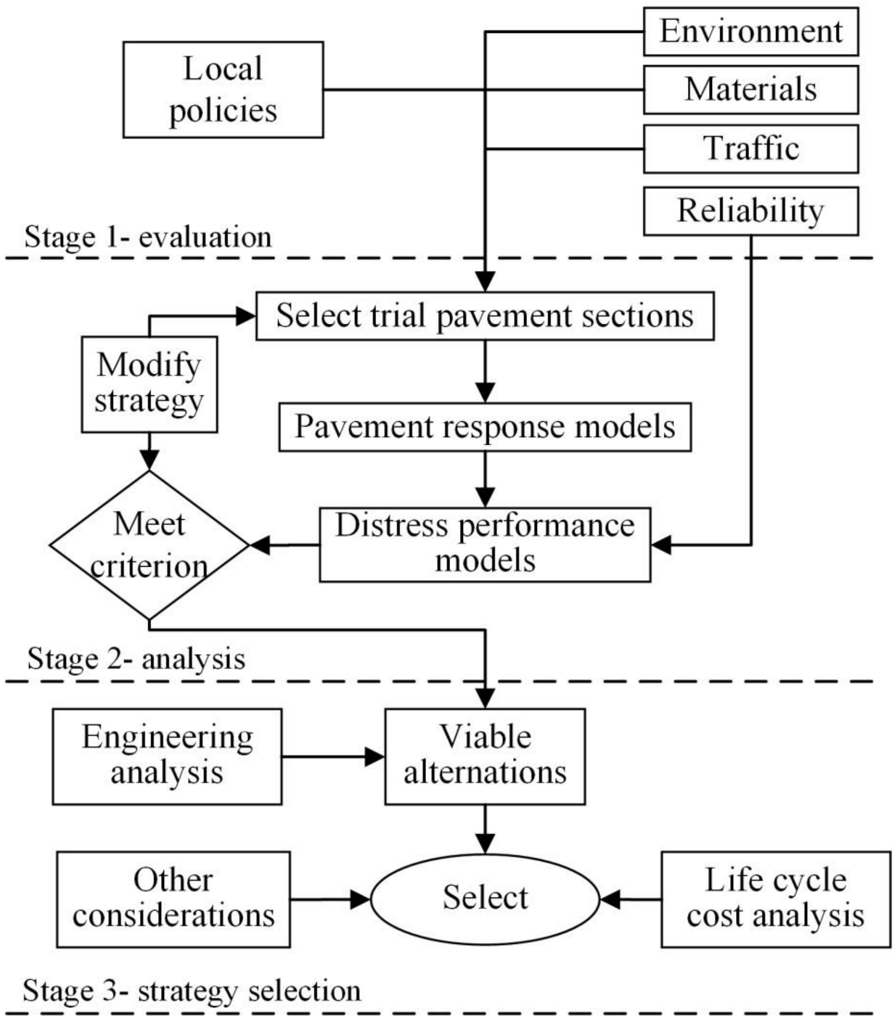

Figure2-2 Flow diagram of design Procedure (Li et al. 2011)

2.2.1 MEPDG Software

Based on design guide procedure, the MEPDG design guide also provides users with user friendly computational software (Version 0.7 resulted from NCHRP 1-37A), which has been updated many times since 2005 (Waseem 2013). NCHRP project 1-40 was an independent, comprehensive review of the MEPDG. It further updated this software and made it more user friendly by developing versions 0.8 and 0.9. The MEPDG software version 1.0 was further improved in 2012 under NCHRP Project 9-30A (VonQuintus et al. 2012).

A typical set of MEPDG pavement design data consisting of material, traffic, and climate data generates over 100 input variables for the project compared with an empirical method with only limited inputs. In this innovative method, some factors neglected before, such as vehicular inputs and climatic changes, are taken into account for both pavement designs and performance predictions (NCHRP 2004).

The mechanistic module of rigid pavement design in the MEPDG is based on the plate theory to calculate stresses in the pavement structure with these inputs. Elastic relationships are used to calculate strains, which are conducted in the empirical module to obtain the incremental damage over time. Transfer functions are employed to convert the mechanistic response to the distress performance predictions.

These prediction models need calibrated coefficients to synchronize distress predictions based on the regional material, climate, traffic data, and local policies. The coefficients in these prediction models are adjusted until the distress predictions are the same as the observed distresses; this process is called local calibration. A database for calibration was the major topic in the NCHRP Project 9-30 report. The goal was to provide an organized database for adjusting M-E based transfer functions' coefficients or calibrating the distress prediction models embedded in the empirical module. With the help of this database, errors generated from the differences between the distress observations and predictions can be reduced.

2.2.2 Hierarchical Design Input Levels

The hierarchical input is a unique characteristic in the MEPDG, which allows the design to be run with different levels of precision in available data. Basic inputs such as traffic, materials, and pavement conditions are all classified in three hierarchical input levels (NCHRP 1-40A 2006):

- Level 1 represents the highest level of input accuracy. These input values are directly obtained from the field and thus, would have the lowest uncertainty. Level 1 input is used for site features, materials, or traffic conditions that are different from the data of another source. Obtaining these inputs demands expensive experimentation and therefore, they are only used when data failure could cause high economic risks.
- Level 2 provides an intermediate level of accuracy. These inputs are gained through correlations or regression equations which are based on experimental Level 1 databases. Input Level 2 also represents regional data provided by local agencies.

•Level 3 is the lowest level of accuracy of input parameters. It is employed where there are minimal consequences of early failure. These are the regional or global default values. This level should only be used for low volume, low risk roads (NCHRP 2004).

Hierarchical input levels should be highlighted due to its efficiency and cost effectiveness. They help in reducing the cost of material testing during a field investigation of pavement site. Input levels can be selected depending upon the economic importance of the pavement structure (Waseem 2013).

2.2.3 Rigid Pavement Distresses

There are different ways for a jointed plain concrete pavement (JPCP) to respond to both the traffic and environment that can affect its initial and long-term performance. Three main types of response are related to traffic and environment. (Bautista et al. 2008)

•Curling stress-Slab curling is caused by a temperature gradient between the top and bottom surfaces of the concrete slab. Stresses are developed in the slab with the weight and friction effectiveness.

•Shrinkage/Expansion-Variation of atmosphere temperature causes JPCP slabs to expand (when hot) and contract (when cool) which leads to joint horizontal movement as well as to curling.

•Load stress-Compressive and tensile stresses are found due to the traffic loads are applied on the JPCP.

The most common structural failure types such as transverse cracking and joint faulting, happening in JPCPs are listed as following along with potential causes (NCHRP 2004).

One of the main distresses is transverse (fatigue) cracking, which results primarily from heavy loading combined with a lack of uniform base support or weak subgrades, expansive soils, and differential settlement. Severe cracking can lead to fragmented and broken up slabs. The total cracking distress prediction (percent slabs cracked) incorporates both bottom-up and top-down cracking rates. Bottom-up transverse cracking occurs when there exists a high positive temperature gradient through the slab (i.e., the top of the slab is warmer than the bottom of the slab). Under this weather condition, repeated applications of heavy traffic will result in fatigue damage at the bottom of the slab, with the greatest damage typically occurring near the slab edge closest to the applied load. As for top-down transverse cracking, the fatigue damage starts from the top of the slab because of the presence of a negative temperature gradient (i.e., the top of the slab is cooler than the bottom of the slab) and repeated traffic acting simultaneously on both ends of the slab (Mu et al. 2012).

Figure 2-3 Illustration of the Faulting and Cracking

The other primary distress type is faulting, which is considered as a major contributing factor to slab cracking and eventual breakup. Faulting is a vertical displacement of abutting slabs at the transverse joints creating a "step" in the pavement, Figure 2-3. It results from the erosion of base material at the transverse joints, and leads to the incomplete and non-uniform support while creating an unpleasant ride. Factors affecting the development of faulting include repeated truck axles crossing transverse joints, the condition of joint load transfer efficiency (LTE), and the presence of fine aggregates and free moisture under the joint LTE is provided by aggregate interlock capacity along the joint, dowels, and the support of the base and concrete shoulder, which is influenced by whether the shoulder is tied or untied.

2.3 Local Calibration of MEPDG

2.3.1 Global Calibration

In the MEPDG, pavement distress prediction models are the key parts of the design and analysis method. The accuracy of any performance prediction model depends on the selection of coefficients in the transfer functions, which is the process of calibration and validation. Consequently, it is imperative that performance prediction models be properly modified or calibrated prior to adopting and using them for design purposes.

The term calibration means the mathematical process through which the total error (often termed residual) between observed and predicted values of distress is minimized (AASHTO 2012). The term validation, however, refers to the process of confirmation in which the calibrated model can produce robust and accurate predictions for cases other than those used for model calibration. A successful validation will make the bias and precision of the model to be similar to those obtained during calibration. This calibration-validation process is critical for users who want to utilize the MEPDG in their pavement design.

The objective of calibration is to obtain a set of coefficients in transfer functions that can minimize the bias between the predicted and observed values of distress. The error function is defined as the sum of squares of the difference between the predicted and measured values of distress, as shown in Equation 2-1. The error minimization procedure is obtained by an iterative process.

$$\mathrm{Error}(C_1, C_2, \cdots C_n) = \sum_{i=1}^{N} (Distress_{prediction}(i) - Distress_{measurement}(i))^2 \tag{2-1}$$

Where:

Error = error function;

$C_1, C_2, \cdots C_n$ = calibration coefficients;

$\mathrm{Distress}_{measurement}$ (i) = measured distress for ith observation in data set;

$\mathrm{Distress}_{meprediction}$ (i) = predicted distress for ith observation in data set;

N = number of observations in data set.

All performance models within the MEPDG were calibrated on a global level by using the Long Term Pavement Performance (LTPP) test sections, which were located in various sites under different conditions across North America. Test sections were also supplemented with performance data from pavements at the Minnesota Road Research Facility, the FHWA Rigid Pavement Performance and Rehabilitation study, and from other sources that included the AASHO Road Test, regular Interstate pavements, and Vandalia test sections. There are only seven rigid pavement LTPP test sections in Canada, none of which are in Ontario.

Historically, calibrations of the MEPDG included all available pavement sections with reliable data. It is assumed that a more robust prediction will be obtained by increasing the number of projects used in the calibration as a result of the larger range of variables included (Sachs 2012).

The number of projects from each source for JPCP calibration, according to Sachs, is broken down as follows: 381 LTPP sections, 9 Minnesota Road Research Facility sections, and 8 AASHO Road Test sections.

Factorial designs are generated and populated with the data set above for performing a global rigid pavement performance model calibration. The transverse fatigue cracking and joint faulting models for the JPCPs were calibrated with projects classified by three separate factorial groups. The factorial designs were conducted to make sure the database included a wide range of conditions in North America.

2.3.2 Needs for Local Calibration

After the completion of NCHRP Project 1-37A, another plan was developed for state highway agencies (SHAs) by AASHTO to implement the MEPDG. Main points in this plan included developing guides and tools to help users to calibrate the distress performance model to satisfy the local conditions, such as materials, traffic, and weather conditions. These guides were the AASHTO MEPDG Local Calibration Guide, and the professional/commercial grade software tool based on the MEPDG design and analysis principles.

All prediction models in the MEPDG were nationally calibrated using representative testing sites around North America, in accordance with the *Guide for the Local calibration of Mechanistic-Empirical Pavement Design Guide*. Most of these testing sites belonged to the LTPP program due to their consistency in the monitored data over time and diversity of location throughout North America.

However, policies on pavement preservation and maintenance, construction, material specifications, and materials vary across the United States and Canada; moreover, they have significant impacts on pavement distress and performance. These factors are not taken into account in the MEDPG but can be influenced by the local calibration parameters embedded in the MEPDG obtained through local calibration.

After the application of the MEPDG across the United States, AASHTO realized the necessity of local calibration of the software and recommended that SHAs should conduct local calibration of the models before fully implementing the MEPDG (FHWA 2010).

Many state agencies in the US had either conducted or planned to undertake local calibration studies for their pavement conditions as that of 2010. In this review, the methodology and achievements of these SHAs are reviewed, including the main approach of local calibration and state-of-art in the local calibration (AASHTO 2010).

The MTO decided to adopt the MEPDG as the new pavement design tool in the future; therefore, there was an urgent need to do the calibration by modifying the factors in the transfer functions of the MEPDG to meet design conditions in Ontario, Canada. For flexible pavement, in recent years, several efforts have been invested in calibration. In 2010, a project funded by MTO HIIFP developed a database for local calibration of MEPDG based on the MTO's Second Generation of MTO PMS performance data and historical contract documents. The initial results indicated that the MEPDG transfer models, particularly for cracking and rutting, needed to be local calibrated urgently (Hamdi 2015). In 2013 and 2015, another two projects funded by MTO HIIFP focused on local calibration of asphalt concrete pavement distress models for Ontario conditions. Relevant studies had analyzed factors affecting pavement performance. (Gulfam.2016). minimized residual errors between the predicted and observed results in cracking models (Ahmed et al. 2016), reduced the indeterminacy of prediction results for rutting models (Gautam.2016), and improved prediction precision of locally calibrated International Roughness Index (IRI) coefficients

(Ayed and Tighe. 2015, Gulfam. 2017).

2.3.3 Procedures for Local Calibration

Based on the Guide for the Local calibration of Mechanistic-Empirical Pavement Design Guide (AASHTO 2010), there are eleven steps to a procedure for local calibration, which are listed as follows.

Step 1—Select Hierarchical Input Level for Each Input Parameter

The first step of the process is to select the hierarchical input level for the inputs that will be used by an agency for pavement design and analysis. In this step, the likely policy should be determined by the actual conditions and testing capabilities, material and construction specifications, and traffic data collection procedures and equipment.

Step 2—Develop Local Experimental Plan and Sampling Template

The second step is to expand a detailed plan or sampling template to refine the calibration of the MEPDG distress and IRI prediction in terms of local conditions, policies, and materials.

Step 3—Estimate Sample Size for Specific Distress Prediction Models

This step is to figure out the size of data set for calibration to confirm the adequacy of the global calibration coefficients.

Step 4—Select Segments

This step is used to select roadway projects to obtain maximum benefit of existing information and data to keep sampling and field testing costs to a minimum.

Step 5—Extract and Evaluate Distress and Project Data

This step of is to collect all data and identify any missing data elements that are needed for the MEPDG.

Step 6—Conduct Field and Forensic Investigations

In order to enhance the accuracy of the local calibration, some typical pavement sections of the most common used materials and structures are be identified.

Step 7—Assess Local Bias

Validation of Global Calibration Values to Local Conditions, Policies, and Materials. The MEPDG global calibration models should be used to calculate the performance indicators for each segment (new pavement and rehabilitation strategies). Then, assess the comparison to determine bias and the standard error of the estimate to validate each distress prediction model for local conditions, policies, specifications, and materials.

Step 8—Eliminate Local Bias of Distress and IRI Prediction Models

The process used to eliminate the bias found to be significant from using the global calibration values depends on the cause of the bias and accuracy desired by the highway agencies.

Step 9—Assess the Standard Error of the Estimate

Compare the standard error determined from the sampling template to the standard error derived from the global data set.

Step 10—Reduce Standard Error of the Estimate

If the standard error is too large, resulting in overly conservative designs at higher reliability levels, revisions to the local calibration values of the transfer function may be needed.

Step 11—Interpretation of Results, Deciding on Adequacy of Calibration Parameters

The local standard error of the estimate (SEE) for each distress models should be evaluated to determine the impact on the resulting designs at different reliability levels.

This process can be modified as needed to meet the local conditions in accordance with approaches being used. For example, in Arizona and Iowa, the procedure above was condensed, including:

- Selection of hierarchical input levels;
- Development of experimental design and sampling needs;
- Selection corresponding projects to populate sampling;
- Forensic investigation;
- Assessment of bias and goodness of the global models and performance of calibrated models;
- Evaluation and reduction the standard errors and determine the precision of the new model.

In Iowa, the process also included seven steps as follows (Ceylan et al. 2013):

- Step 1: Update and tabulate the Iowa pavement system database for Pavement ME Design local calibration.
- Step 2: Conduct Pavement ME Design runs using (1) national and (2) MEPDG local calibration coefficients identified in InTrans Project 11-401.
- Step 3: Evaluate the accuracy of both nationally and MEPDG-locally calibrated pavement performance prediction models.
- Step 4: If the accuracy of national or MEPDG local calibration coefficients for given Pavement ME Design performance prediction models were found to be adequate; these coefficients were determined to be acceptable for Iowa conditions.
- Step 5: If not, the calibration coefficients of Pavement ME Design can be refined using various optimization approaches.
- Step 6: Evaluate adequacy of refined Pavement ME Design local calibration coefficients.
- Step 7: Recommend Pavement ME Design calibration coefficients for Iowa conditions.

It should be noted that, according to NCHRP 1-37A, the standard error associated with the distress prediction model will decrease as the engineering input level increased. This will logically lead to the reduction of life-cycle costs, overall.

2.3.4 Sensitivity Analysis

Sensitivity analysis (SA) is important in the process of local calibration. The sensitivity of performance models to calibration coefficients was analyzed to: (1) to derive how the values of calibration coefficients affect prediction results, and (2) make subsequent calibration coefficient optimization more efficient by identifying the changes in performance predictions in relation to changes in calibration coefficients (Ceylan 2013).

Generally, knowledge of the sensitivity of base cases, design inputs, sampling methodology, analysis execution, response surface modeling, and sensitivity metrics to the design input values can help the designer identify which is the most influential factor to predicted performance in the specific climatic regions or under traffic conditions. Moreover, it can help them decide where additional effort should be taken to provide higher efficiency input (Schwartz et al. 2011).

The sensitivity analysis was developed to find the proper coefficients for the transfer function. This method can be described as trial-and-error, which means that each time a performance prediction is calculated, the error of the measurement is also calculated. The results can be achieved after enough repeats have been performed to eliminate the error bias and reduce the standard error of the estimate. The key point of applying this method for local calibration is to find proper metrics that can be used to quantify the sensitivity of model outputs to inputs. According to Schwartz's report, the primary metric for the sensitivity analyses is a point-normalized sensitivity index. One-at-a-time (OAT) sensitivity analysis is a usual way to quantify the sensitivity of each transfer equation coefficient, which can determine the scope of change in the output as the response to a difference in only one input at a time (NCHRP 2011). A coefficient sensitivity index (S_{ijk}) and a coefficient-normalized sensitivity index (S_{ijk}^{N}) were adopted to describe the effects on joint faulting prediction in terms of the changes in each calibration coefficient.

The coefficient sensitivity index (S_{ijk}) can be calculated as follows:

$$S_{ijk} = \frac{\partial y_j}{\partial x_k} \cong \frac{\triangle Y_j}{\triangle X_K} = \frac{Y_{j,i+1} - Y_{j,i}}{X_{k,i+1} - X_{k,i}} \qquad (2\text{-}2)$$

Where:

$Y_{j,i}$ = the values of the performance prediction j evaluated at global calibration coefficient condition i in a model,

$X_{k,i}$= the values of calibration coefficient k evaluated at global calibration coefficient condition i in a model.

For each calibration coefficient,X_k two coefficient sensitivity indices S_{ijk}were calculated using, e.g. 20 % increased and 20 % decreased values of calibration coefficients ($X_{k,1.2i}$ > $X_{k,i}$ and $X_{k,0.8i}$ <$X_{k,i}$). As for the comparison of coefficient sensitivity, the indices should be normalized.

$$S_{ijk}^{N} = \frac{\partial y_j}{\partial x_k} \cong \frac{\triangle Y_j}{\triangle X_K} \frac{X_{ki}}{Y_{ji}} \qquad (2\text{-}3)$$

Based on this sensitivity analysis, a hierarchy can be determined in terms of their influence on the values of JPCP transfer functions.

Usually, finding the proper set of coefficients is a process of combining sensitivity analysis and mathematical optimization. There are two types of transfer functions found in the software, namely functions being used to calculate the performance prediction directly, and the functions being used to obtain incremental damage over time. In the first case, a nonlinear optimization technique is applied through MS Excel® Solver or LINGO® to minimize the bias (ε) and the mean square error (MSE) between the actual measurements and the prediction values (Velasquez et al. 2009, FHWA 2010a, Jadoun 2011). This approach demands all the components required by the performance models to achieve closed form solution provided by the MEPDG. Thus, the method can make it possible to find proper coefficients to meet the calibration demands by using the mathematical optimization technique, which helps the users to develop prediction models with these components separately from the MEPDG.

When some components are not provided by the software for the prediction, for example, the number of axle loading and an allowable number of axle loading in the cracking-model, the prediction models cannot be run independently from the MEPDG. Therefore, these prediction models cannot be closed between inputs and outputs to be able to employ conventional optimization methodologies (Ceylan et al. 2013). In this case, many runs are needed to determine transfer function coefficients through a trial-and-error procedure. A linear optimization approach using the sensitivity index is developed as a screening method to reduce the burden of the trial-and-error. The individual bias (ε_{ijk}) of each calibration coefficient per distress model is calculated. This is done by taking the weight partition of total bias (ε_t) of all calibration coefficients per performance prediction, determined from coefficient normalized sensitivity index (S_{ijk}^N) as:

$$\varepsilon_{ijk} = \varepsilon_t \times S_{ijk}^N \tag{2-4}$$

Suppose the predicted value of performance (i), $y_i^{measured} \approx y_i^{local-predicted}$. It will be:

$$\varepsilon_{ijk} = y_i^{local-predicted} - y_i^{global-predicted} \quad (2\text{-}5)$$

$$S_{ijk} = \left.\frac{\Delta Y_j}{\Delta X_K}\right|_i = \frac{\varepsilon_{ijk}}{x_k^{local} - x_k^{global}} \quad (2\text{-}6)$$

$$x_k^{local} = x_k^{global} + \frac{\varepsilon_{ijk}}{S_{ijk}} \quad (2\text{-}7)$$

The locally calibrated pilot coefficient x_k^{local} is an approximate solution assuming a linear relationship between the calibration coefficient and prediction. The trial-and-error procedure by running MEPDG based on the pilot coefficient x_k^{local}- aims to match the solution closely.

This approach was employed to figure out the local calibration coefficients of the models when the mathematical optimization was not able to meet the accuracy demand of local calibration. It should be noted that overestimation of performance prediction can lead to a more conservative design approach as there is not much difference of bias compared to underestimation of predictions (Ceylan et al. 2013).

2.3.4 Performance Indicators and Distress Performance Models

There are three types of JPCP distress prediction models involved in the MEPDG, including transverse cracking, faulting, and pavement roughness (IRI). The components of each model will determine the corresponding results and the techniques used in the local calibration.

Transverse Cracking Model

In rigid pavements, transverse cracking is caused by repeated loading (AASHTO 2010). Under typical service conditions, transverse cracking can occur starting at either the top or bottom of the concrete slab due to slab curling. The potential for either mode of cracking may be present in all slabs.

Bottom-Up cracking happens when a tensile bending stress occurs at the bottom of the slab under the wheel load. This stress develops greatly with a high positive temperature gradient through the slab (the top of the slab is warmer than the bottom of the slab). Top-Down cracking happens when the pavement exposed to negative temperature gradients (the top of the slab cooler than the bottom of the slab) is subject to fatigue damage at the top of the slab. Equation 2-8 shows the prediction of transverse cracking for both top-down and bottom-up models.

$$\mathrm{CRK} = \frac{100}{1+C_4(DI_F)^{-C_5}} \tag{2-8}$$

Where:

CRK = predicted amount of bottom-up and top-down cracking (fraction);

$\mathrm{DI_F}$ = fatigue damage which is calculated by the following model.

The equation of the fatigue model is as shown in the following equation 2-9.

$$\mathrm{DI_F} = \sum \frac{n_{i,j,k,l,m,n}}{N_{i,j,k,l,m,n}} \tag{2-9}$$

Where:

$n_{i,j,k,m,n,o}$ = applied number of load at condition of i,j,k,l,m,n;

$N_{i,j,k,m,n,o}$ = allowable number of load at condition of i,j,k,l,m,n.

The applied number of load application n is based on traffic conditions, design life, and temperature differentials throughout the slab. However, the allowable amount of loads depends on the applied stress and the strength of the slab, and can be expressed as Equation 2-10.

$$\log(N_{i,j,k,l,m,n}) = C_1 \left(\frac{M_{Ri}}{\sigma_{i,j,k,l,m,n}}\right)^{C_2} \tag{2-10}$$

Where:

M_{Ri} = PCC modulus of rupture at age i, Mpa;

$\sigma_{i,j,k,l,m,n}$ = applied stress at condition of i,j,k,l,m,n,

C1, C2, C4, C5 are the calibration coefficients of the model.

In the models of transverse cracking, any slab can crack from either the bottom or the top of the concrete pavement, but not both simultaneously. Therefore, the predicted bottom-up and top-down cracking are combined in such a way where both types of cracking are reported, but the possibility of both modes occurring on the same slab is excluded. So the total cracking prediction is calculated by summing each of bottom-up and top-down cracking together by using Equation 2-11.

$$T_{crack} = \left(CRK_{bottom-up} + CRK_{top-down} - CRK_{bottom-up} \cdot CRK_{top-down}\right) \cdot 100\% \qquad (2\text{-}11)$$

Where:

T_{crack} = total transverse cracking (percentage);

$CRK_{bottom-up}$ = predicted the amount of bottom-up transverse cracking;

CRK_{top-up} = predicted the amount of top-up transverse cracking.

To calibrate the cracking model, according to M. Darter, the researchers investigated the reason for the poor goodness fit and bias of using global factors. They found the factors C1 and C2 are related to substantial field testing data, hence, changing them is not recommended (AASHTO 2008).

Joint Faulting

The joint faulting is predicted on a monthly basis using an incremental approach. A faulting increment is determined each month, and the current faulting level affects the magnitude of the increase. The faulting at each month is determined as a sum of faulting increases from all previous months in the pavement life from the traffic opening date using the following equations:

$$\mathrm{Fault}_m = \sum_{i=1}^{m} \Delta\,\mathrm{Fault}_i \qquad (2\text{-}12)$$

$$\Delta\,\mathrm{Fault}_i = C_{34} \cdot (\mathrm{FaultMAX}_{i-1} - \mathrm{Fault}_{i-1})^2 \mathrm{DE}_i \qquad (2\text{-}13)$$

$$\mathrm{FaultMAX}_i = \mathrm{FaultMAX}_{i-1} + C_7 \cdot \mathrm{DE}_i \cdot \log(1 + C_5 \cdot 5.0^{\mathrm{EROD}})^{C_6} \qquad (2\text{-}14)$$

$$\mathrm{FaultMAX0} = C_{12} \cdot \delta_{\mathrm{curling}}\left[\log(1 + C_5 \cdot 5.0^{\mathrm{EROD}}) * \log\left(\frac{P_{200}\mathrm{WetDays}}{P_s}\right)\right]^{C_6} \qquad (2\text{-}15)$$

Where:

$Fault_m$ = Mean joint faulting at the end of month m;

$\Delta Fault_i$ = Incremental change in mean joint faulting during month I;

$FaultMAX_i$ = Maximum mean joint faulting for month I;

$FaultMAX_0$ = Initial maximum mean joint faulting;

$EROD$ = base/subbase erodibility factor;

$\delta_{curling}$ = Maximum mean monthly slab corner upward deflection due to curling and warping;

DE_i = Differential density of energy of subgrade deformation accumulated in month i;

P_s = Overburden on the subgrade;

P_{200} = Percent of subgrade material Passing #200 sieve;

$WetDays$ = Average annual number of wet days.

C1, C2, C3, C4, C5, C6, C7, C12, C34 = calibration coefficients:

$$C_{12} = C_1 + C_2 * FR^{0.25} \tag{2-16}$$

$$C_{34} = C_3 + C_4 * FR^{0.25} \tag{2-17}$$

Where:

FR = base freezing index defined as the percent of the time the top base temperature is below 0°C (32°F).

From the equations above, it can be seen the faulting predictions are related to several variables, such as joint, temperature, and modulus of the base layer. For each incremental month, the temperature difference can be obtained throughout the PCC slab for each hour using the Integrated Climate Module (ICM) embedded in the MEPDG. In terms of the temperature gradient and the base modulus, the curling and warping of the slab are determined for each month. Thus, the faulting at each month is determined as a sum of faulting increments of all previous months in the pavement's life since opening; the performance models are shown as the Equation 2-14. The faulting increment is determined each month, as shown in Equation 2-15.

It should be noted that all the metrics above are in imperial units due to the primary units of the performance model, and the imperial system is only converted to metric after analysis has been concluded.

IRI model

In the MEPDG, smoothness or pavement roughness (IRI) is a function of the first as-constructed profile of the pavement and any change in the longitudinal profile over time due to distresses and foundation movements. The global IRI model was calibrated and validated by using LTPP field data under a variety of climatic and field conditions. The equation is shown as follows:

$$\mathrm{IRI} = IRI_0 + C_1 * CRK + C_2 * SPALL + C_3 * TFault + C_4 * SF \tag{2-18}$$

Where:

IRI = predicted IRI value (m/km);

IRI_0 = initial smoothness measured as IRI;

CRK = percent of slabs with cracking (fraction);

SPALL = percentage of joint with spalling (medium and high severity);

TFault = total joint faulting accumulated per km;

C1, C2, C3, C4 = the calibrated coefficients.

$$\mathrm{SF} = \mathrm{AGE} * (1 + 0.5556 \cdot \mathrm{FI}) * (1 + \mathrm{P}_{200}) * 10^{-6} \tag{2-19}$$

AGE = pavement age, year;

FI =freezing index, ℉ · days;

P_{200} = percent subgrade material passing through No200 sieve.

$$\mathrm{SPALL} = \left(\frac{AGE}{AGE + 0.01}\right) \cdot \left(\frac{100}{1 + 1.005^{-12 * AGE + SCF}}\right) \tag{2-20}$$

Where:

SCF = scaling factor based on site design, and climate related.

2.4 Local Calibration Efforts and Challenges

According to *Implementation of The AASHTO Mechanistic-Empirical Pavement Design Guide and Software* (Pierce 2014), a survey was developed to evaluate the efforts of US, Puerto Rico, and Canadian state highway and provincial transportation agencies in relation to the MEPDG. Since March 2013, 57 agencies (90%) responded to the survey, including 47 U.S. highway agencies, Puerto Rico, and nine Canadian provincial and territorial governments. As for the local calibration in these agencies, two aspects were identified as important, namely consistency of distress definitions and thresholds set by agencies.

The key step in the local calibration process is evaluating how well the MEPDG predicted pavement performance (i.e., distress and IRI) corresponds to observed field performance (AASHTO 2010). By comparison, the agency is able to determine if local calibration of the prediction models is necessary or the performance prediction models are adequate.

But before making the comparison, agency pavement performance measurements need to be consistent with the corresponding denotation in the Distress Identification Manual (AASHTO 2010). If the agency distress definitions are different from those used in the MEPDG (AASHTO 2008), they should be revised to agree with the terms in Distress Identification Manual (AASHTO 2010). The survey also showed most agencies indicated that IRI (40 agencies), rut depth (38 agencies), and alligator cracking (36 agencies) data were consistent with the Distress Identification Manual.

As for JPCP, agencies in the survey reported that transverse cracking (35 agencies) and faulting (33 agencies) were consistent with the LTPP method, and so was a punchout measurement for agencies that constructed Continuous Reinforced Concrete Pavement (CRCP).

Table 2-2 Default performance criteria and reliability in the MEPDG

Performance Criteria	Limit	Reliability
Flexible Pavement		
Initial IRI (m/km)	1	N/A
Terminal IRI (m/km)	2.7	90
Longitudinal cracking (m/km)	3.8	90
Alligator cracking (percent)	25	90
Transverse cracking(m/km)	0.5	90
Rigid Pavement		
Initial IRI (m/km)	1	N/A
Terminal IRI (m/km)	2.7	90
JPCP transverse cracking (percent slabs)	15	90
JPCP mean joint (mm)	5	90
CRCP punchout (number per km)	10	90

Before conducting the local calibration, the agency should define the threshold limits and reliability limits for each of the performance prediction models according to local policies and conditions. Those default performance criteria and reliability levels for asphalt and concrete pavement that could be changed in MEPDG are listed in Table 2-2. Table 2-3 provides the Ontario performance threshold limits and reliability levels for asphalt and concrete.

Table 2-3 Performance criteria and reliability in Ontario (MTO 2014)

Performance Criteria		Limit	Reliability
Flexible Pavement			
Initial IRI (m/km)	Freeway	0.8	95
	Arterial	1	Urban:90,Rural:85
Terminal IRI (m/km)	Freeway	1.9	95
	Arterial	2.3	Urban:90,Rural:85
Longitudinal cracking (m/km)	Freeway	380	95
	Arterial		Urban:90,Rural:85
Alligator cracking (percent)	Freeway	10	95
	Arterial	20	Urban:90,Rural:85
Rigid Pavement			
Initial IRI (cm/km)	Freeway	1.3	95
	Arterial	1.5	Urban:90,Rural:85
Terminal IRI (cm/km)	Freeway	2.4	95
	Arterial	2.7	Urban:90,Rural:85
JPCP transverse cracking (percent slabs)	Freeway	10	95
	Arterial	15	Urban:90,Rural:85
JPCP mean joint (mm)	Freeway	3	95
	Arterial		Urban:90,Rural:85

In addition, there are two research programs sponsored by the FHWA in the US that have been conducted on using PMS data for local calibration of MEPDG. The study, which was named "Using Pavement Management Data to Calibrate and Validate the New MEPDG, An Eight State Study" (FHWA 2006a, FHWA 2006b), focused on the potential use of PMS for local calibration. Eight States got involved in this study, including Florida, Kansas, Minnesota, Mississippi, New Mexico, North Carolina, Pennsylvania, and Washington. The study concluded that all States studied could employ PMS data for MEPDG calibrations and this was likely true for other states not involved in the study.

The other study, named FHWA HIF-11-026 "The Local Calibration of MEPDG Using PMS" (FHWA 2010a, FHWA 2010b), was to develop a framework for using existing PMS data to calibrate performance models. North Carolina was selected on screening criteria to finalize and verify the MEPDG calibration framework based on a set of actual conditions (Kaya 2015). With this developed framework, local calibration for the selected states was demonstrated under the assumptions of both MEPDG performance predictions and distress measurements from a selected state. Studies on pavement performance prediction model primarily focused on new JPCP, including the work by Li et al. (2006) in Washington, Schram and Abdelrahman (2006) in Nebraska, Darter et al. (2009) in Utah, Velasquez et al (2009) in Minnesota, Titus-Glover and Mallela (2009) in Ohio, Mallela et al. (2009) in Missouri, Kim et al. (2010) in Iowa, Bustos et al. (2009) in Argentina, Delgadillo et al. (2011) in Chile, Li et al. (2011) in Washington, Mallela et al. (2013) in Colorado, and Darter et al. (2014) in Arizona.

For rigid pavements, the calibrated models, such as cracking, faulting and IRI model, have been calibrated in many states in the US and had better results compared to global models. Examples of the local calibration were in Washington, Minnesota, Colorado, Iowa, and Arizona (Table 2-4. Table 2-5).

Table 2-4 Calibration efforts of flexible pavement taken by agencies

Country	Agency	Longitudinal cracking	Alligator Cracking	Thermal cracking	Rut depth		Reflective cracking	IRI
					Asphalt layer	Total		
U.S.A	Arizona	√	√	Global	Global	√	√	√
	Colorado	√	√	√	√	√	√	√
	Hawaii	Future	Future	Future	Future	Future	Future	√
	Indiana		√	Global	Global			√
	Missouri	Global	Global		√	√	Global	√
	New Jersey	Future	Future	Future	Future	Future	Future	√
	Oregon	√	√	√	√	√	Global	√
Canada	Ontario	√	√	√	√	√	√	√

In Washington State, the calibrated transverse cracking model and the local calibration coefficients provided a better prediction as compared to the global model. Some significant local calibration coefficients for their pavement sections were found in the calibration data set. The SHA also tried different calibration coefficients to apply to both un-dowelled and dowel-bar pavements.

Table 2-5 Calibration efforts of rigid pavement taken by agencies

Country	Agency	JPCP			CRCP	
		IRI	Transverse cracking	Faulting	IRI	Punchouts
U.S.A	Arizona	√	√	√	√	√
	Colorado	√	√	√		
	Florida	√	√	√		
	Indiana	√	Global	Global		
	Missouri	√	Global	Global		
	North Dakoda	√	Global	Global		
	Oregon	√	Global	Global		
Canada	Ontario				√	√

An iterative approach was used to calibrate the transverse cracking model in Minnesota locally. This recalibration was conducted using the performance data from MnROAD pavement cells as well as the LTPP test sections within the state. The calibrated coefficients improved the transverse cracking predictions for the pavement sections in the calibration set, and no adjustment of the faulting model was recommended (Brink 2015). It should also be noted that the model was calibrated on a limited data set.

State Highway Agencies (SHA) in Colorado found that their JPCP pavement sections were performing well and did not show any significant difference in cracking model. Consequently, they did not conduct the calibration for the transverse cracking model.

In Iowa, the calibrated transverse cracking model for JPCP gave better predictions with lower bias and standard errors than the global model. It improves the accuracy of predictions by tightening the scatter along the line of equality, compared with the overestimated global IRI values.

Overall, the locally calibrated JPCP performance prediction models (faulting, transverse cracking, and IRI) are recommended in Iowa as alternatives to their globally calibrated counterparts. More important, Iowa provides an efficient way of optimization for local calibration, which applied non-linear and linear methods to determine coefficients of transfer functions to reduce many software runs.

Local calibration in Arizona showed the transverse cracking model reflected the changes in the measurement of the coefficient of thermal expansion (CTE). The updated CTE measurements resulted in slightly lower values with similar methods as the original global calibration.

Table 2-6 Calibration results of rigid pavement of some parts of the US

Coefficients	MEPDG	Arizona	Colorado	Florida	Missouri
Cracking					
C1	2.0	2.0	2.0	2.8389	2.0
C2	1.22	1.22	1.22	0.9647	1.22
C4	1.0	0.19	0.6	0.564	1.0
C5	-1.99	-2.067	-2.05	-0.5946	-1.99
Faulting					
C1	1.0184	0.0355	0.5104	4.0472	1.0184
C2	0.91656	0.1147	0.00838	0.91656	0.91656
C3	0.002848	0.00436	0.00147	0.002848	0.002848
C4	0.000883739	1.1e-07	0.008345	0.000883739	0.000883739
C5	250	20000	5999	250	250
C6	0.4	2.309	0.8404	0.079	0.4
C7	1.8331	0.189	5.9293	1.8331	1.8331
C8	400	400	400	400	400
IRI					
C1	0.8203	0.6	0.8203	0.8203	0.8203
C2	0.4417	3.48	0.4417	0.4417	1.17
C3	1.4929	1.22	1.4929	2.2555	1.43
C4	25.24	45.2	45.2	25.24	66.8

SHA in Kansas calibrated the faulting model coefficient for three different chemically stabilized base types. The calibration coefficients were adjusted for all three base types. Depending on the results, the locally calibrated models showed lower Squared Error of Estimate (SEE) compared to the global model. Similarly to the transverse cracking model, the globally calibrated faulting model was re-calibrated to reflect the changes in the CTE measurements.

The global model was accepted in Ohio and Missouri, since there was no significant difference observed between the measured and predicted transverse cracking. As W. C. Brink had pointed, both studies in these two states recommended applying the local calibration of the model once more condition data becomes available for the selected projects. (Brink 2015)

The local calibration coefficients for the rigid pavements performance models adopted by various SHA's are shown, Tables 2-6. It can be observed from these tables that significantly different coefficients are possible in a region or state as compared to the coefficients in the global models.

Up to now nearly all the agencies in the US and Canada indicated that some or all of the MEPDG performance prediction models had been calibrated to local conditions. Depending on the performance prediction model, reported calibration coefficients varied significantly.

2.5 Current Calibration Progress in Ontario

Over the past few years, several HIIFP programs have been conducted to support the local calibration of MEPDG for flexible pavement in Ontario (Yuan 2015). However, due to the difficulties of this project, the current study has achieved only limited success, besides the pavement database for local calibration. The further research aims to promote the current level of local calibration by using more accurate field measurements and forensic investigations (Yuan 2015).

A 2010-11 HIIFP project developed a database for local calibration of MEPDG based on the MTO's PMS2 (the Second Generation of MTO PMS) performance data and historical contract documents. A few preliminary calibration studies were performed with this database. Results from the initial calibration proved the urgent need for MEPDG local calibration, particularly for rutting and cracking models.

Table 2-7 Calibration results of flexible pavement in Ontario

Distress	Coefficient	Global	Local
Rutting	β_{AC}	1	2.357
	β_{GB}	1	0.1254
	β_{SG}	1	0.2482
Alligator cracking	C1	1	0.9186
	C2	1	0.0095
	C4	6000	6000
Longitudinal cracking	C1	7	5.556
	C2	3.5	-0.2839
IRI	C1	40	5.927
	C2	0.4	0.4
	C3	0.008	0.008
	C4	0.015	0.018

Another project started in 2013 to conduct local calibration by using an expanded database that includes different types of asphalt concrete. The rutting models have achieved some limited results; similarly, several other local calibration methods were also developed, although not all of them could reduce the bias and residuals efficiently. These methods, however, are based on several fundamental assumptions. For example, one of them was the layer contribution to the overall surface rut depth, but real trench investigations are required to address this issue thoroughly.

Extensive research has been performed since 2009 to develop a local calibration database based on MTO's PMS-2 for the further application in the future (Wassem 2013). The latest local calibration results have been achieved, including the cracking and rutting models for Ontario's new and rehabilitated flexible pavements. Table 2-7 gives the details about the new findings.

2.6 Summary of Chapter

Currently, the MEPDG has been used in the United States and some Canadian Provinces as the standard design method. As an innovative method for pavement design, it may predict the performance using various prediction models. However, due to the difference in weather, materials, and traffic, local calibration of the MEPDG is necessary for the implementation in Ontario. The AASHTO has provided guidelines for local calibration, and many examples are shown how to conduct local calibration. The procedure of these examples will be helpful to overcome the challenges in local calibration.

The primary goal of local calibration is to determine the calibration coefficients of prediction models under local conditions and reduce the bias and standard error of predictions by comparing to the forensic measurements. Based on the literature review, the main problem that should be overcome in the process of research is how to choose a proper optimization procedure. A common method is the trial-and-error approach in local calibration guide (AASHTO 2010), which requires many MEPDG runs to adjust coefficients of transfer functions gradually. Some relevant research works have been conducted to improve this situation to make the calibration effort efficient (Kaya 2015). The research will discuss the right mathematical methods to make the performance prediction agree with the actual measurements.

CHAPTER 3 RESEARCH METHODOLOGY

3.1 Introduction

The main objectives of this chapter are to (a) outline the overall methods of the local calibration; (b) highlight various factors related to the data preparation for Ontario calibration, and (c) provide an appropriate procedure to calibrate the model for use in Ontario.

The MEPDG contains three separate empirical transfer models for distress prediction in the JPCP structures. The three models include transverse cracking, faulting, and IRI models with 15 coefficients.(AASHTO 2010)

Table 3-1 Coefficients in the distress transfer function

Performance Item	Transfer Functions	Coefficients
Transverse Cracking	$\log(N_{i,j,k,l,m,n}) = C_1 (\frac{M_{Ri}}{\sigma_{i,j,k,l,m,n}})^{C_2}$ $CRK = \frac{100}{1 + C_4 (DI_F)^{-C_5}}$	C1,C2,C4,C5
Mean Faulting	$FaultMAX0 = C_{12} \cdot \delta_{curling}[\log(1 + C_5 \cdot 5.0^{EROD}) * \log(\frac{P_{200}WetDays}{P_s})]^{C_6}$ $FaultMAX_i = FaultMAX_{i-1} + C_7 \cdot DE_i \cdot \log(1 + C_5 \cdot 5.0^{EROD})^{C_6}$ $\Delta Fault_i = C_{34} \cdot (FaultMAX_{i-1} - Fault_{i-1})^2 DE_i$ $Fault_m = \sum_{i=1}^{m} \Delta Fault_i$ $C_{12} = C_1 + C_2 * FR^{0.25}$ $C_{34} = C_3 + C_4 * FR^{0.25}$	C1,C2,C3,C4,C5,C6,C7
Smooth roughness (IRI)	$IRI = IRI_1 + C_1 * CRK + C_2 * SPALL + C_3 * TFault + C_4 * SF$	C1,C2,C3,C4

The NCHRP 1-40D and 1-47 (NCHRP 2006b, 2011) guides are the main references for the practice of local calibration for the MEPDG performance models. These guides outline the primary steps of the calibration process and general methods for local calibration. Additionally, the guides demonstrate that the objectives of calibration are to (a) confirm that the models can predict pavement distress and IRI without bias, and (b) minimize the Residual Sum of Squares (RSS) associated with the transfer functions. The RSS demonstrates the scatter of the data along the line of equality between predicted and measured distress. Therefore, RSS is the key indicator to evaluate the results in the local calibration and can be expressed as shown below. For a specific pavement section j with observed total distress Distress_j and calculated predicted permanent value $Prediction_j$ at different inspection time, the RSS is defined as

$$\text{RSS} = \sum_{j=1}^{n} (Distress_j - Prediction_j)^2 \tag{3-1}$$

According to AASHTO local calibration guide, there are eleven steps of the procedure to achieve the local calibration results (AASHTO 2010). However, previous studies showed the procedures could be modified to satisfy their own local conditions. For example, the procedures for local calibration in Iowa pavement systems was made. Based on the relevant literature review (Ceylan et al. 2013), a set of procedures for local calibration in Ontario was developed to satisfy the need of the local agency. The procedures are listed as following steps:

- Step 1, Select pavement sites represent pavement at different geographical locations and different traffic levels
- Step 2, Conduct the MEPDG runs using national calibration coefficients
- Step 3, Evaluate the accuracy of both nationally calibrated pavement performance prediction models
- Step 4, If the accuracy of global prediction models is found to be adequate, these coefficients are determined to be acceptable for local conditions.
- Step 5, If not, the calibration coefficients can be refined using various optimization approaches
- Step 6, Evaluate adequacy of refined the local calibration coefficients
- Step 7, Recommend MEPDG calibration coefficients for local conditions.

3.2 Influential factors for Local Calibration

A group of pavement sections representing local pavement design, construction practices, and performance should be selected to build a database for the local calibration. However, developing such a database is a challenging task, when only limited real data is available, and LTPP sections are absent in Ontario, as is the case for the rigid pavement. Developing a database includes five steps: (1) Determining the minimum number of pavement sections based on the statistical requirements; (2) Identifying all available in-service pavement projects constructed after 1990; (3) Extracting all pavement distresses from the MTO's database for all identified projects; (4) Collecting traffic, climate, structural and material data for these sections; and (5) Evaluating the measured performance for all the identified projects

Inputs related to traffic, climate, design and material characterization should cover a wide range, as these factors have great influence on local calibration.

3.2.1 Determine the Minimum Number of Pavement Sections

The minimum number of pavement sections for local calibration is based on statistical needs. The NCHRP 1-40B provides an approach to determine the minimum number of sections for each performance measure. The minimum number of sections is calculated by Equation 3-2, and the results are summarized in Table 3-2 for each performance measure.

Table 3-2 Minimum number of sections for local calibration of Ontario

Indicators	Performance Threshold (at 90% reliability)	Tolerable Bias	Global Standard Error of Estimate(SEE)	Minimum Number of section required
Transverse Cracking	10%(freeway) 15%(arterial)	7.2	4.52%	11
Joint Faulting	3 mm	2.5	0.84mm	13
Initial IRI	Freeway:1.3; Arterial: 1.5			
Terminal IRI	2.7 m/km	4.2	0.27m/km	100

$$n = \left(\frac{Z_{\alpha/2}\sigma}{e_t}\right)^2 \tag{3-2}$$

Where:

n = Minimum number of pavement sections;

σ = Performance threshold;

e_t = Tolerable bias $Z_{\alpha/2}$ * global model SEE.

3.2.2 Description of Selected Pavement Sections

A total of 32 pavement sections were chosen for the local calibration of rigid pavements.

Listed below are few factors concerning the selections that were taken into account.

Table 3-3 Information of the Selected Roads

REGION	DISTRICT	HWY	Current AADTT	LENGTH	Construction year
Eastern	Bancroft	115	1900	2.693	1991
Eastern	Bancroft	115	1920	1.990	1991
Eastern	Bancroft	115	1920	11.622	1990
Eastern	Bancroft	115	1920	3.000	1990
Eastern	Bancroft	115	1920	4.532	1989
Eastern	Bancroft	115	2020	3.500	1989
Eastern	Ottawa	417	1452	34.390	2002
Eastern	Ottawa	417	1812	34.390	2004
West	Chatham	401	10756	10.470	2006
West	Chatham	401	10756	10.470	2006
West	Chatham	401	10250	9.910	2006
West	Chatham	401	10134	9.910	2006
West	Chatham	401	10250	7.160	2009
West	Chatham	401	10250	7.160	2009
West	Chatham	401	10134	10.250	2007
West	Chatham	401	10134	10.250	2007
West	Chatham	401	10134	4.120	2008
West	Chatham	401	10134	4.120	2008
West	Chatham	3	1160	4.900	2000
West	Chatham	3	1454	6.674	2010
West	Chatham	3	1284	7.340	2008
West	Chatham	3	1470	7.340	2008
West	Chatham	402	6400	11.300	2007
West	Chatham	402	6262	11.300	2007
Central	Toronto	404	3268	6.410	2014
Central	Toronto	404	3268	6.410	2014
Central	Toronto	404	3268	5.400	2014
Central	Toronto	404	3268	5.400	2014
Central	Toronto	401	27300	3.898	2010
Central	Toronto	401	27300	3.898	2010
Central	Toronto	401	25300	3.898	2010
Central	Toronto	401	25300	3.898	2010

•Site factors: The site factors addressed the various regions in Ontario.

•Traffic: According to the statistics, there are 12 sections with less than 1000 AADTT, 15 sections with AADTT between 10000 and 30000, and none more than 30000 AADTT.

•Thicknesses: The range of constructed PCC thicknesses.

•Open to traffic date: The information is needed to determine the performance period.

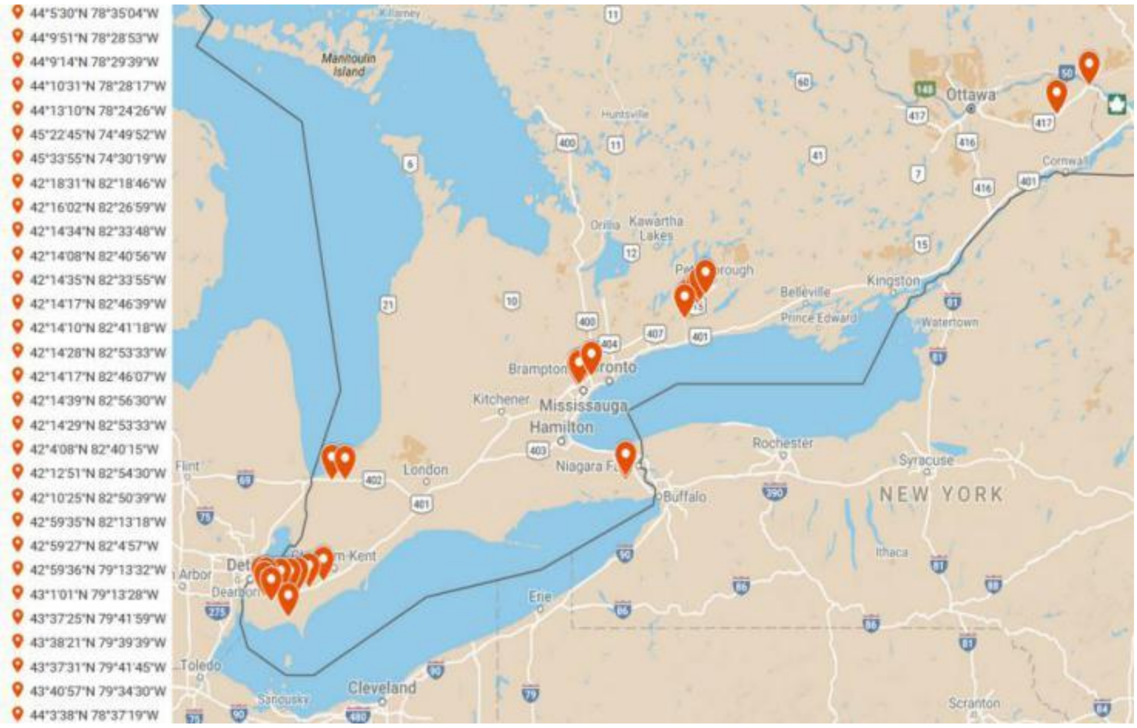

Figure 3-1 Locations of the selected roads (Google Map 2017)

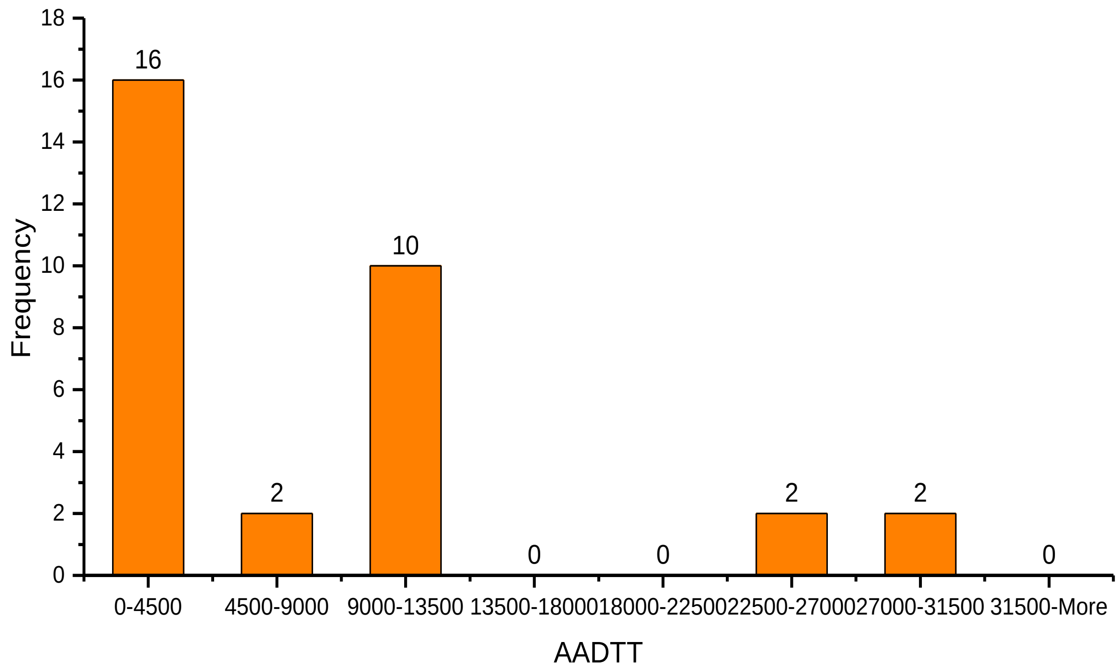

Figure 3-2 Selected Pavements distribution by Average Annual Daily Truck Traffic (AADTT)

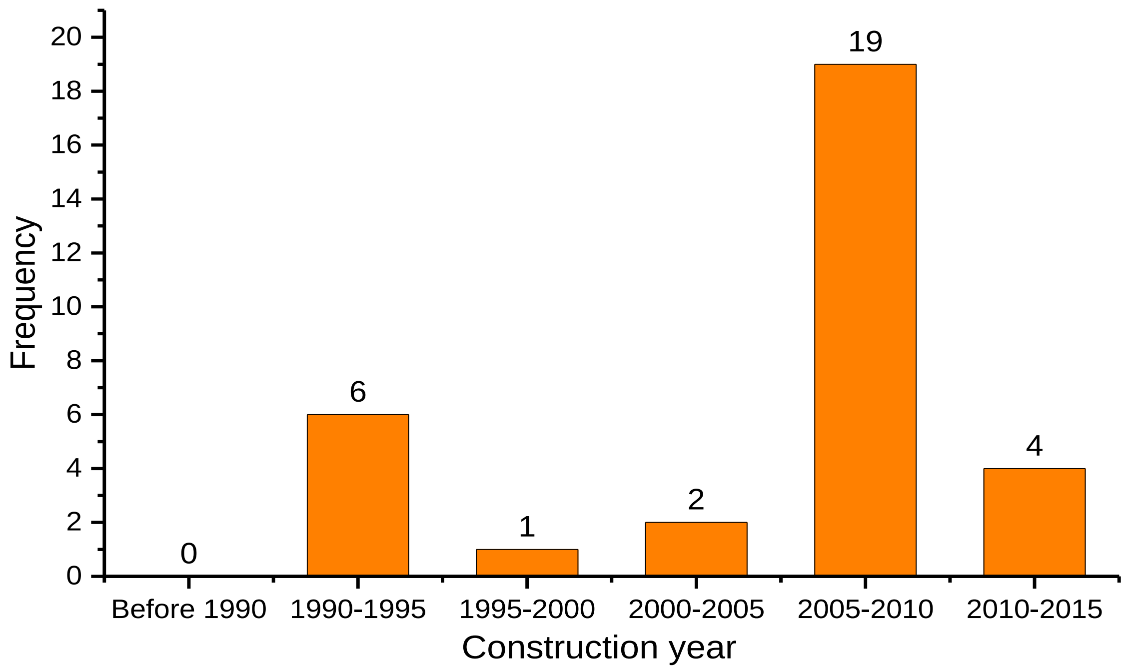

Figure3-3 Selected Pavements distribution by Construction Year

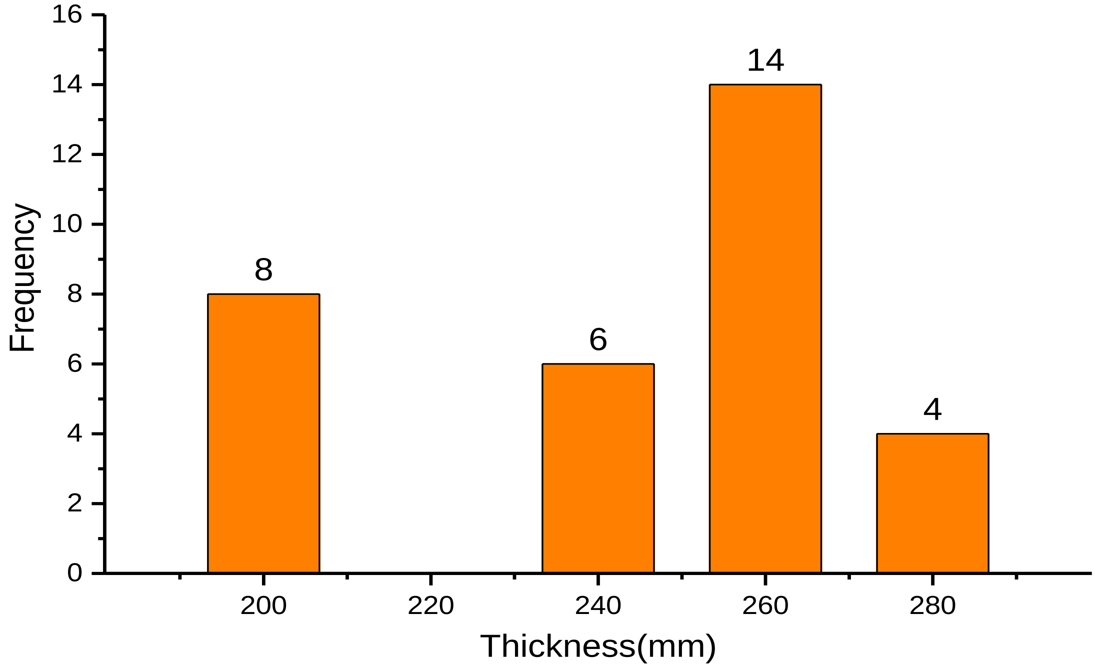

Figure3-4 Selected Pavements distribution by Thickness

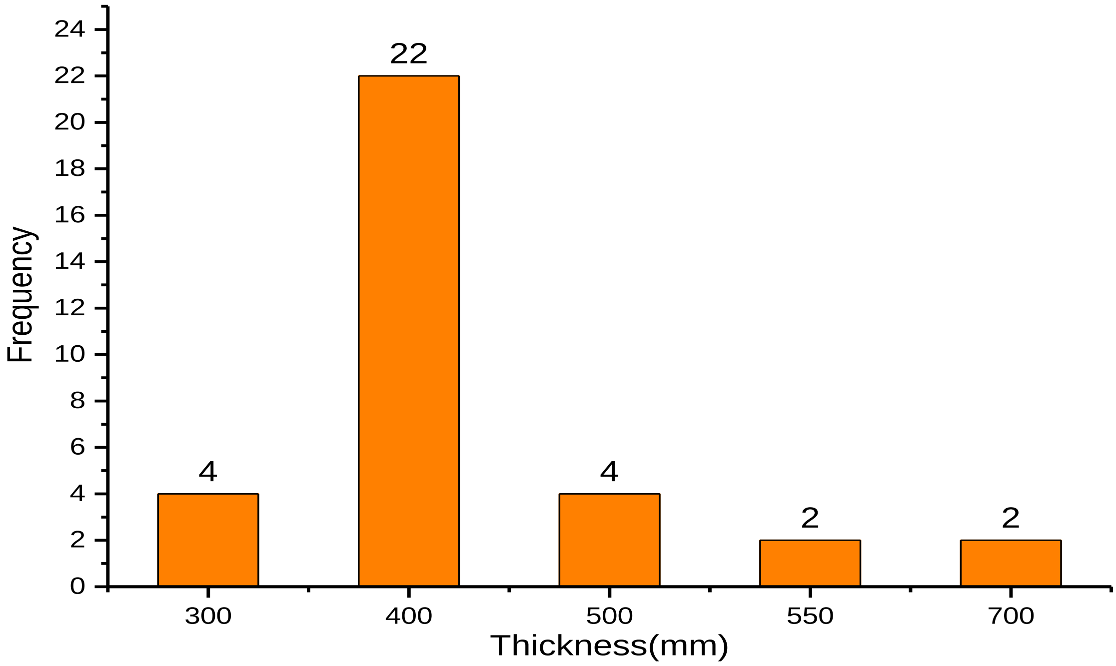

Figure3-5 Selected Pavements distribution by Base Thickness

Figure3-1 presents a variety of geographical locations across Ontario, and Figure3-2 demonstrates the average annual daily truck traffic distribution (AADTT). The structure thickness of surface and base for each pavement are presented in Figure3-4 and Figure 3-5.

3.3 Pavement Database

3.3.1Traffic Inputs

The traffic inputs for the MEPDG are generated on the basis of FHWA traffic statistical method, which requires five basic types of traffic data: (1) AADTT, (2) vehicle class distribution, (3) axle load spectrum, (4) axle configuration and spacing, and (5) monthly/hourly adjustment factors. A list of default axle load distribution for various facility types are embedded in the software, but they may not reflect the conditions in Ontario. Therefore, a web-based mapping program, called iCorridor, was developed by MTO in terms of the Commercial Vehicle Survey (CVS) data. The iCorridor system provides site-specific traffic data such as AADTT, vehicle class distribution, the number of axle per truck, and axle load distribution. These traffic data are available for users to view or download the traffic data on the interface of the section. Figure 3-5 shows an example of the iCorridor interface for traffic data. The default MEPDG values or the values recommended by NCHRP 1-47A reports (NCHRP 2011) are used in the case that the values were not available on the website.

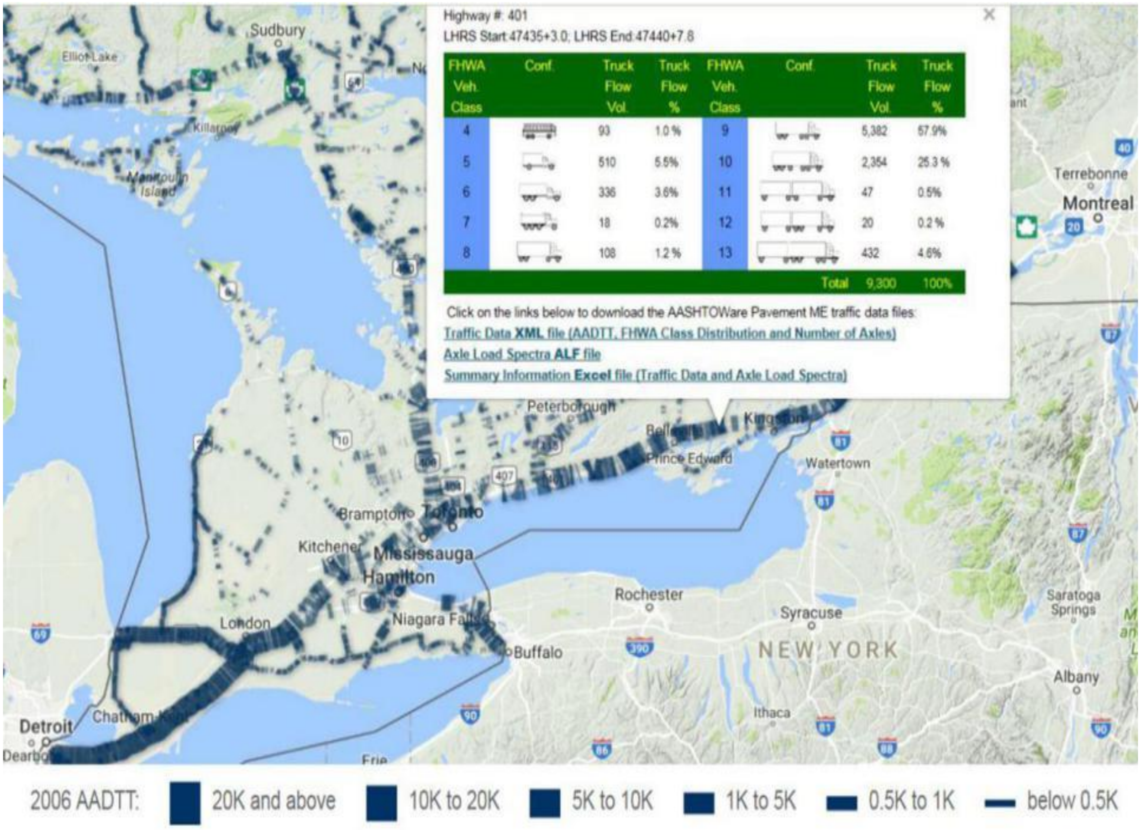

Figure 3-6 iCorridor Map Interface for Traffic Data

3.3.2 Climate Inputs

The MEPDG software has incorporated climate data at weather stations across North America. It can also generate climate data by extrapolating the data from nearby weather stations if the latitude and longitude are known. For instance, if the specific location of selected sections obtained from MTO PMS was input, the climate data of each section could be generated. There is a total of 34 weather stations in Ontario used for this purpose, and their data is updated periodically. Figure 3-7 shows the locations and names of the 34 weather stations in Ontario. The weather station located nearby should be chosen, or if there is no such station, the interpolation function will be applied in processing the data from neighboring stations.

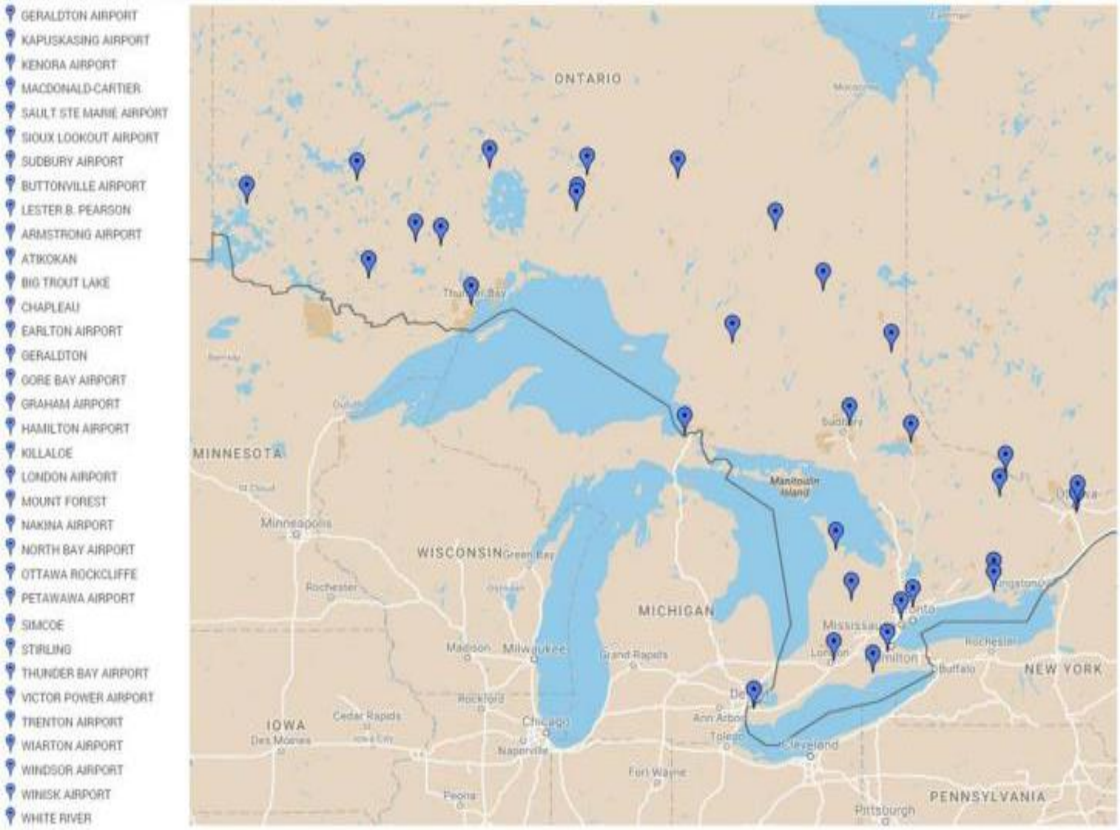

Figure 3-7 Weather Stations for MEPDG Calibration in Ontario

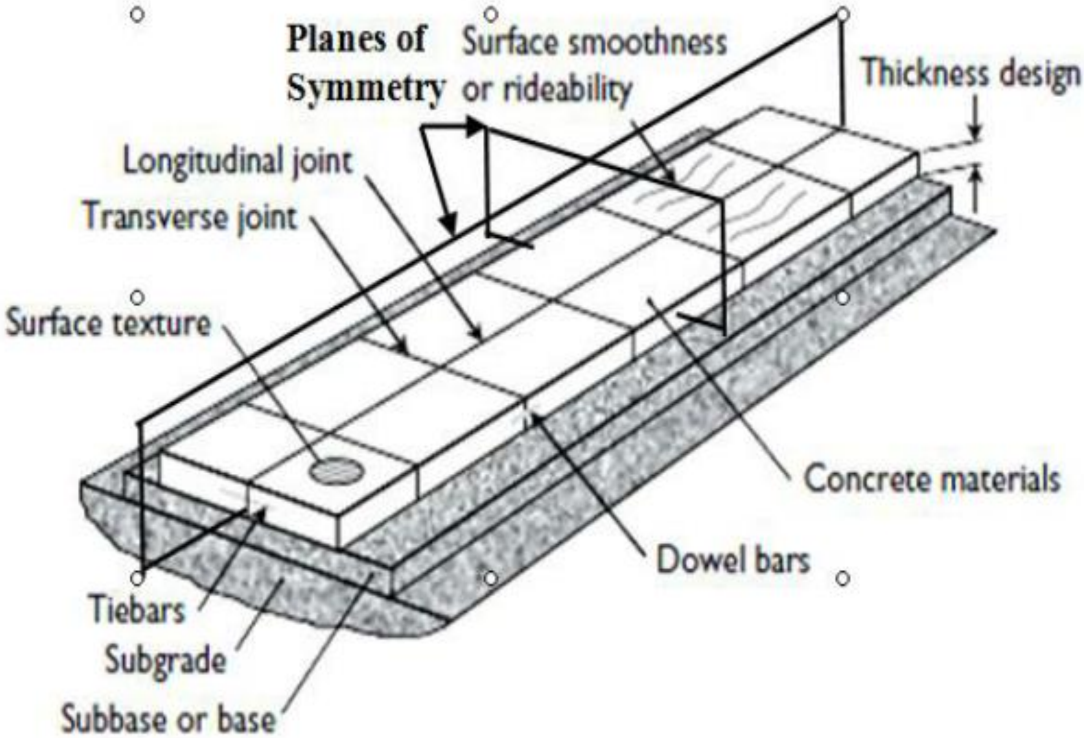

Figure 3-8 Schematic Diagram of a Jointed Plain Concrete Pavement (Rahman 2014)

3.3.3 Material and structure inputs

Concrete pavement used in Ontario should meet the requirements of the Ontario Provincial Standard Specification (OPSS 350). JPCP (Figure 3-8) with dowelled joints and widened slabs is popular in Ontario. The primary material properties and parameters (default values) of a typical concrete pavement are given in Table 3-4 (MTO 2014).

Units of the MTO distress surveys of transverse cracking are not consistent with those of the MEPDG performance predictions. For example, in MTO's PMS the cracking is expressed as the length of the distress while in MEPDG it is expressed as the percentage of cracked slabs.

For calibration of performance prediction models, these measured values of distress in PMS are converted into the same metrics as those of the predictions in the MEPDG.
Assumptions to convert the MTO values to units consistent with the MEPDG are made as follows:

1) the width of a lane is 3.6 m;
2) all the measured values of cracking will be summed up no matter how serious;
3) joint spacing is 3.5m, 4m, 4.3m, 4.5m (random);
4) it is a full-length transverse cracking.

The total crack quantity was divided within certain pavement section length by the width of the slab to get a cracking count. The total number of slabs within the pavement section can be estimated using the design slab length. In this way, the slab crack percentage was obtained on the assumption that there was only one transverse crack per slab. For example, if a sum of every magnitude of transverse crack is 72m, the number of cracks will be 72/3.6=20. A formula to calculate cracking was developed as Equation 3-3.

$$T_c = \frac{Total\_Cracking\_Ext}{Length/joint\_spacing \times width} \tag{3-3}$$

Where:

$Total\_Cracking\_Ext$ = Length of transverse cracks, m;

$Length$ = Section length, m;

$joint\_spacing$ = The distance between two joints;

$width$ = Width of each slab.

Table 3-4 Ontario typical concrete material and structural design Parameters

PCC material Properties		JPCP slabs and Joints Parameters	
Item of Parameter	Value	Item of Parameter	Value
Cement Type	GU (Type 1)	Thickness of slabs (mm)	Project specific
Cementious Material Content(kg/m3)	335	Unit Weight (kg/m^3)	2320
Water/Cement Ratio	0.45	Poisson's Ratio	0.2
Aggregate Type	Limestone	PCC Joint Spacing (m)	3.5,4,4.3,4.5 (random)
Reversible Shrinkage (% of Ultimate Shrinkage)	50%	Sealant Type	Other
Time to Develop 50% of Ultimate Shrinkage (Day)	35	Spacing of Dowels at Joints (mm)	300
PCC 28 Day Compressive Strength (Mpa)	38 (≥30)	Diameter of Dowels at Joints (mm)	32
PCC 28 Day Modulus of Rupture (MPa)	5.6	Widened slab (m)	4.25
PCC Elastic Modulus (Mpa)	29,600	Tied Shoulders	Tied with long term load transfer efficiency of 70
PCC Coefficient of Thermal Expansion (mm/mm degC e^{-6})	7.8	Erodibility Index	Very Erodible
PCC Thermal Conductivity (watt/meter-Kelvin)	2.16	PCC-base Contact Friction	Full friction with friction loss at (240) months
PCC Heat Capacity (joule/kg-Kelvin)	1172	Permanent Curl/Warp Effective Temperature Difference (deg C)	-5.6

For local calibration, the distress magnitudes should cover a reasonable range (i.e., above and below threshold limits for each distress type). Therefore, the distress values for all sections were summarized to determine their magnitude ranges. Figure 3-9 presents distributions of transverse cracking and age for the selected JPCP sections. The transverse cracking for all projects ranged from 0 to 5% slabs cracked while no sections exceeded the distress threshold of 15% slabs cracked. The most transverse cracking occurred between the ages of 5 and 15 years.

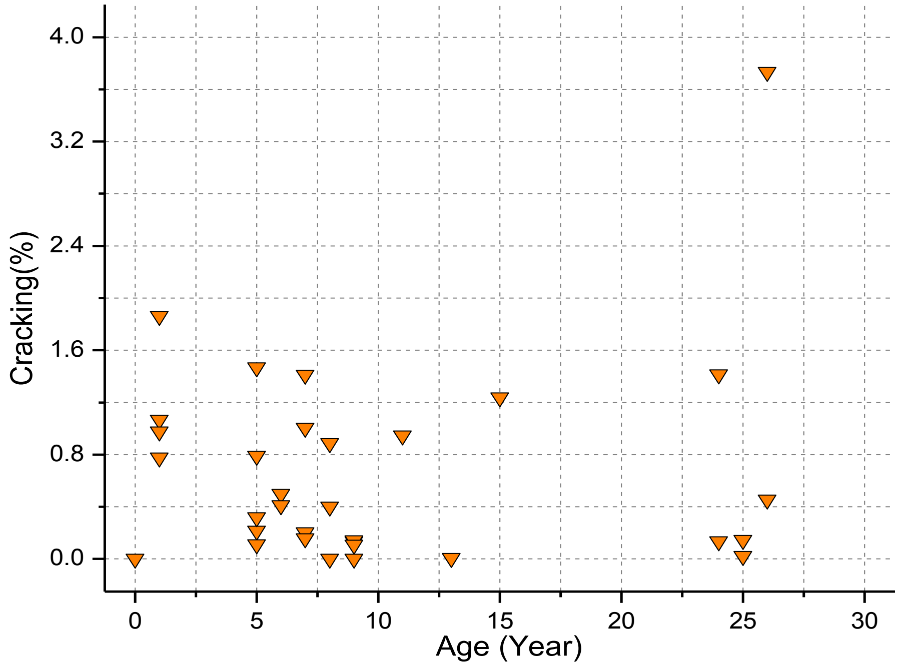

Figure 3-9 Distribution of transverse cracking

As for faulting data, from Figure 3-10 the values of most projects ranged from 0 to 0.7mm, and only one point exceeded the faulting threshold of 3mm. The age at maximum measured values ranged from 5 to 15 years.

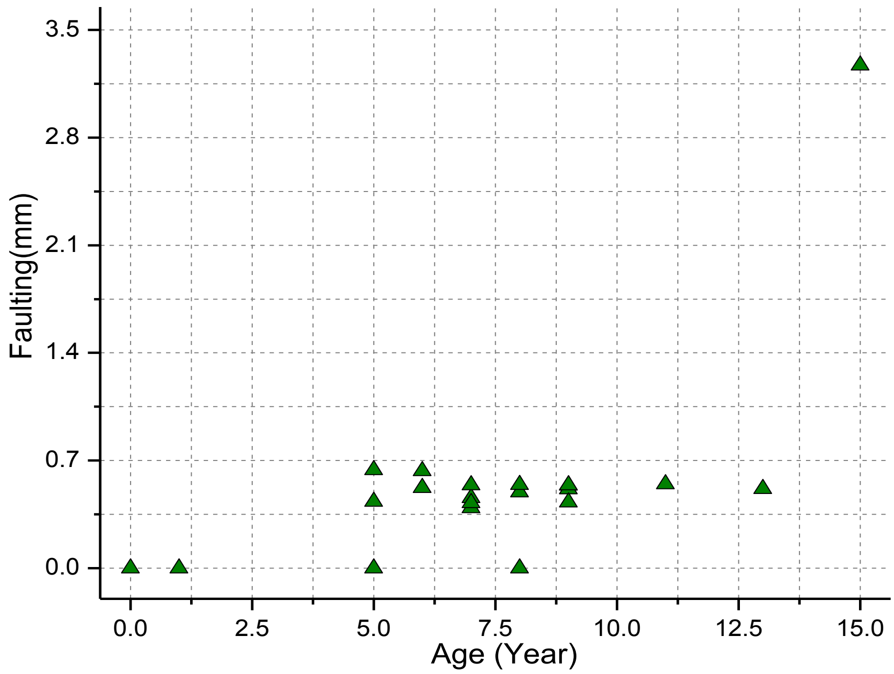

Figure 3-10 Distribution of Faulting

Most of the measured values of IRI were in an interval of 1.2 to 1.8, and corresponding age ranged from 2 to 14 years.

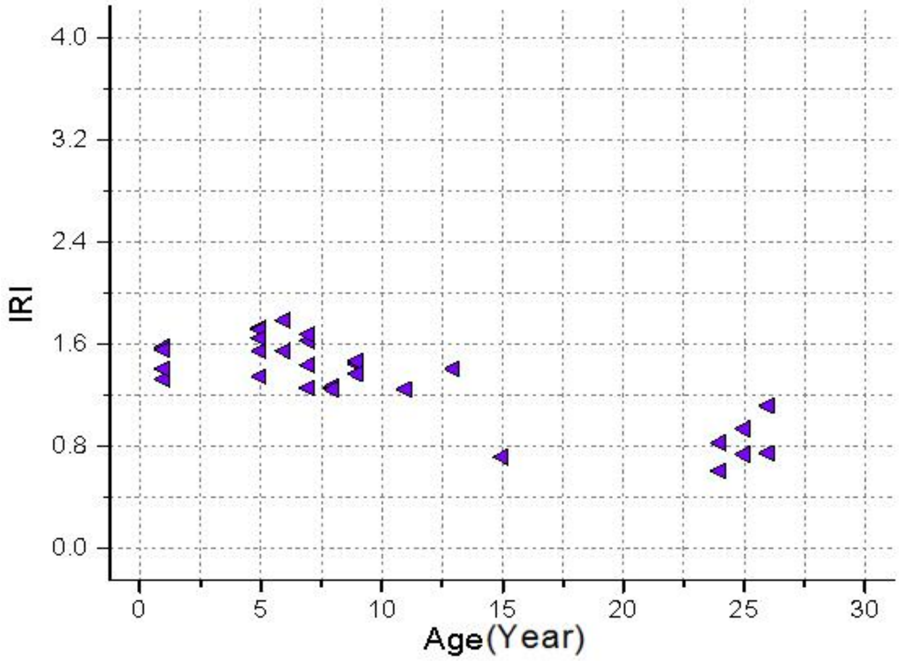

Figure 3-11 Distribution of IRI

3.4 Calibration Procedure

The residual squared sum (RSS) between the predicted values and the actual measured values can be minimized (Ceylan et al. 2013, Kim et al. 2014, Kaya 2015), if all the components in the transfer functions are provided by the software in intermediate files otherwise known to the designer. Thus, the model predictions can be calculated separately from the MEPDG software by using other software like MS Excel® or LINGO®. In this case, calibration of performance models can be done by the non-linear method.

If not all the components of the functions are known, calibration can be conducted only partly by Excel nonlinear solver. For example, because the parameter of allowable repetitions ($N_{allowable}$) is not available in the software or any of its intermediate files, the transverse cracking function coefficients C1 and C2 of the fatigue model is calibrated by the linear method to determine the coefficients in transfer functions. After the two coefficients are determined, the other coefficients (C3 and C4) can be determined by using the nonlinear method. The following table lists all the components in the transfer functions:

Table 3-5 Status of the components in transfer function

Performance Item	Transfer Functions	Availability of components in Transfer function	
Transverse Cracking	$\log(N_{i,j,k,l,m,n}) = C_1 (\frac{M_{Ri}}{\sigma_{i,j,k,l,m,n}})^{C_2}$ $CRK = \frac{100}{1 + C_4(DI_F)^{-C_5}}$	$N_{i,j,k,l,m,n}$	x
		M_{Ri}	x
		$\sigma_{i,j,k,l,m,n}$	x
		DI_F	√
Mean Faulting	$FaultMAX0 = C_{12} \cdot \delta_{curling}[\log(1 + C_5 \cdot 5.0^{EROD}) * \log\left(\frac{P_{200} WetDays}{P_s}\right)]^{C_6}$ $FaultMAX_i = FaultMAX_{i-1} + C_7/10^6 \cdot DE_i \cdot \log(1 + C_5 \cdot 5.0^{EROD})^{C_6}$ $\Delta Fault_i = C_{34} \cdot (FaultMAX_{i-1} - Fault_{i-1})^2 DE_i$ $Fault_m = \sum_{i=1}^{m} \Delta Fault_i$ $C_{12} = C_1 + C_2 * FR^{0.25}$ $C_{34} = C_3 + C_4 * FR^{0.25}$	$\delta_{curling}$	√
		$EROD$	√
		P_{200}	√
		$WetDays$	√
		P_s	√
		DE_i	√
		FR	√
Smooth roughness (IRI)	$IRI = IRI_1 + C_1 * CRK + C_2 * SPALL + C_3 * TFault + C_4 * SF$	CRK	√
		$SPALL$	√
		$TFault$	√
		SF	√

It can be seen from the Table 3-5 that some components of the transfer functions for transverse cracking are not available in intermediate output files. However, the rest have been provided. Consequently, the nonlinear method was employed to seek proper coefficients in most transfer functions, such as faulting, IRI models, and part of the transverse cracking model. (AASHTO 2010).

The commonly used nonlinear solver is provided by MS Excel® which is applied to minimize the RSS and eliminate the bias performance values (Kaya 2015). A number of optimization methods are embedded in MS Excel®, such as generalized reduced gradient (GRG), simplex (Simplex LP), and evolutionary. GRG is used for the non-linear equations, while Simplex LP is only used for linear equations, and Evolutionary can be applied to both non-linear and linear equations. Comparatively, GRG is the most robust and fastest tool for determining the best combination of calibration coefficients (Frontline Systems, Inc. 2017). Other software like LINGO® (LINDO System Inc.) is implemented to find all possible solutions and to see whether any other solutions can satisfy the problem statement due to the limitation of MS Excel® solver on finding all the possible solutions. Meanwhile, LINGO® was also used in this study to check the results produced by MS Excel® solver.

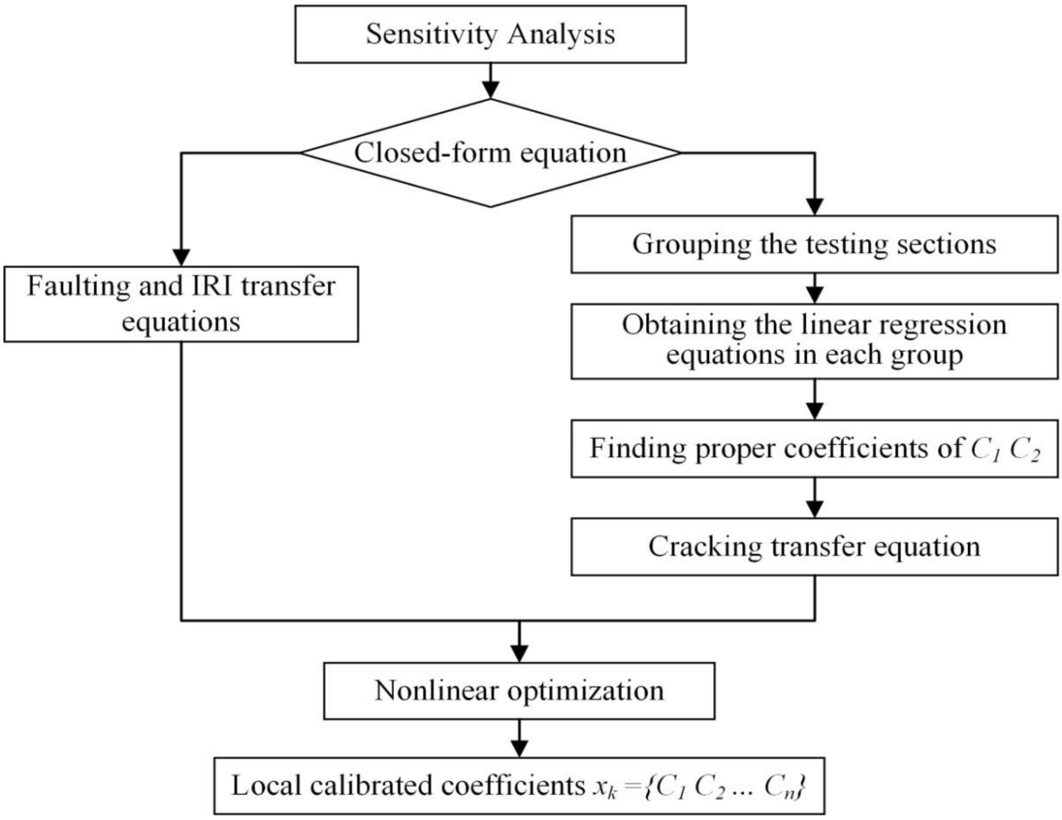

Figure 3-12 Flowchart of local calibration

In this case, the calibration is implemented by non-linear method. However, the nonlinear method cannot be used for the transverse cracking model in a JPCP section. The transfer functions are expressed from Equation 3-4 to Equation 3-6. Several variables like allowable repetition ($N_{i,j,k,l,m,n}$) of axle loading and the accumulative loading ($n_{i,j,k,l,m,n}$) should be known. Up to date version of AASHTOWare does not provide these intermediate values.

$$\log(N_{i,j,k,l,m,n}) = C_1 \left(\frac{M_{Ri}}{\sigma_{i,j,k,l,m,n}}\right)^{C_2} \tag{3-4}$$

$$DI_F = \frac{n_{i,j,l,k,m,n}}{N_{i,j,k,l,m,n}} \tag{3-5}$$

$$\mathrm{CRK} = \frac{100}{1 + C_4 (DI_F)^{-C_5}} \tag{3-6}$$

Where:

CRK = predicted amount of bottom-up and top-down cracking (fraction);

DI_F = fatigue damage;

$n_{i,j,k,m,n,o}$ = applied number of load at condition of i,j,k,l,m,n;

$N_{i,j,k,m,n,o}$ = allowable number of load at condition of i,j,k,l,m,n;

M_{Ri} = PCC modulus of rupture at age i, psi;

$\sigma_{i,j,k,l,m,n}$ = applied stress at condition of i,j,k,l,m,n.

- Step 1, the testing roads are grouped into several types in terms of their traffic and environmental conditions.
- Step 2, a statistical approach is used to find the relation between the coefficients and the fatigue damage DI_F of each type by running the software. The fatigue damage data are collected correspondingly in terms of the change of coefficients C1 and C2.
- Step 3, a linear model in each group is established to calculate fatigue damage through multiple linear regression methods.
- Step 4, an optimization process is employed based on the regression equation of each type of testing roads to minimize the variation of DI_F, which means the deviation of DI_F is minimum. Through this procedure, calibrated C1 and C2 are found with the responding DI_F.
- Step 5, both the bottom-up and top-down fatigue damage of each section can be obtained by inputting the determined coefficients C1 and C2. The values were extracted under the "Cracking Data" tab from the MEPDG output files. So far, all the components in the transfer functions are available in these files.
- Step 6, in Table 3-5, all the coefficients were optimized with the help of the nonlinear optimization approach (MS Excel Solver). In the process of the local calibration, the bias of prediction and the way to determine an optimum are the common problems.

In Step 1, the testing roads are grouped into several types in terms of the location. The fatigue damage values are compared in each group. It can be found that these fatigue values have a great diversity of the section types. The results caused by this diversity will lead to the difference in the transverse cracking values and the discreteness of coefficients.

GRG algorithm was adopted in nonlinear in Excel Solver. However, this algorithm has its limitations in dealing with the problem with more than one feasible region or set of similar values for the decision variables, where all the constraints are satisfied. Within each possible region, there may be more than one "peak" (if maximizing) or "valley" (if minimizing) -- and the solver cannot determine which peak is tallest, or which valley is deepest. In addition, there may be false peaks or valleys known as "saddle points." As a result, this method can make few guarantees about finding the "true" optimal solution. (Frontline Systems, Inc. 2017)

3.5 Assessment of Calibration

The evaluation of the local calibration depends on the comparison with the global calibration results. Predicted performance values were plotted against the observed values for the sections to determine whether or not it was necessary to modify the global coefficient under the conditions in Ontario. If needed, the model coefficients should be modified locally to improve the accuracy of predictions.

By plotting the observed values against the predictions on a 45-degree line of equality, the accuracy of performance predictions was observed intuitively. Meanwhile, the average bias, standard error, and mean absolute percentage error (MAPE) values are assessment indices (Ceylan 2009). The indicators are defined as follows:

$$\text{Average\_Bias} = \varepsilon_{ave} = \frac{\sum_{j=1}^{n}(y_j^{measured} - y_j^{predicted})}{n} \tag{3-7}$$

$$\text{Standard\_Error} = \sqrt{\frac{\sum_{j=1}^{n}(y_j^{measured} - y_j^{predicted})^2}{n}} \tag{3-8}$$

$$\text{MAPE} = \frac{1}{n}\sum_{j=1}^{n}\left|\frac{y_j^{measured} - y_j^{predicted}}{y_j^{measured}}\right| \tag{3-9}$$

Where:

P =number of parameters in the model;

N =number of data points in each distress model;

$y^{measured}$ =measured distress data;

$y^{predicted}$ =predicted distress data;

Several statistical indicators are adopted to evaluate faulting prediction accuracy of both global coefficients and local coefficients. Average Bias (AB) is a quantitative term to demonstrate the average of differences between observed and predicted values, Equation 3-7. Standard Error Estimate (SEE) is defined as the amount of variation or dispersion of a set of the difference between predicted and observed values, Equation 3-8. Mean Absolute Percentage Error (MAPE) depicts the absolute percentage of error to the actual value, Equation 3-9.

A hypothesis test was used to assess the result of calibration to identify whether there was a significant difference between the measurements and predictions. In this test, the following null and alternative hypothesis are assumed:

i. H 0: Mean measured distress = mean predicted distress

ii. H A: Mean measured distress $\neq$ mean predicted distress.

Equation 3-10 is used for the calculation of t values used in these test.

$$t = \frac{(y_j^{measured} - y_j^{predicted})_{mean}}{\frac{S_d}{\sqrt{n}}} \tag{3-10}$$

Where:

n =number of data points;

$y^{predicted}$=predicted distress data;

$y^{measured}$= measured distress data;

S_e =standard deviation of paired data.

This indicator follows t-distribution with n-1 degrees of freedom. If F-value < Threshold (depending on reliability) or P-value > 0.05, this implies that the predictions and measurements are not significantly different on the given reliability. In contrast, if these conditions are not met, then the two data sets can be conserved to be significantly different.

3.6 Summary

In this chapter, local calibration methods have been discussed for rigid pavements. The nonlinear method can be applied in the calibration the faulting and IRI models directly. If the relationship between the fatigue damage and the corresponding coefficients is found, the nonlinear method can also be employed.

Chapter 4 RESULTS OF LOCAL CALIBRATION

4.1 Introduction

This chapter presents the calibration results of 32 JPCP sections using the methodology outlined in Chapter 3. The sections are divided into calibration part (70% sections) and validation part (30% sections). The calibrated models include transverse cracking, joint faulting, and the smoothness (IRI). The detailed steps of calibration for each model are listed, as they can provide a clear instruction for local calibration. Finally, a validation and comparison with results of the models will proceed.

4.2 Transverse Cracking (Bottom-Up and Top-Down)

Two parts are required to be calculated, namely the fatigue damage model and the cracking model. For the given conditions, the number of allowable load repetitions is estimated by the fatigue damage model, and correspondingly equivalent transverse cracking predictions are computed by the transfer function based on the fatigue estimation. The cracking predictions were calculated from a set of equations as follows (AASHTO 2008).

$$\log(N_{allowable}) = C_1\left(\frac{M_R}{\sigma}\right)^{C_2} \tag{4-1}$$

$$T_{cracking} = \frac{1}{1+C_4 \cdot DI_F{}^{C_5}} \tag{4-2}$$

$$\mathrm{DI}_F = \frac{N_{Applied}}{N_{Allowable}} \tag{4-3}$$

Where:

MR = Modulus of rupture of the concrete;

σ = Critical stress in the slab in different cases;

DI_F = Fatigue damage

$N_{Applied}$ = Applied number of load applications;

$N_{Allowable}$ = Allowable number of load applications

$C_{1,2,4,5}$ = Calibration coefficients.

Total transverse cracking value is calculated as follows:

$$T_{cracking} = Crack_{Bottom-top} + Crack_{Top-down} - Crack_{Bottom-top} \cdot Crack_{Top-down} \quad (4\text{-}4)$$

Where:

$T_{Cracking}$ = Total transverse cracking (percent, all severities);

$Crack_{Bottom-up}$ = Predicted amount of Bottom-up transverse cracking (fraction);

$Crack_{Top-down}$ = Predicted amount of Top-down transverse cracking (fraction).

It was found that in the fatigue damage model with two factors, C2 was the most sensitive coefficient, while C4 was the most sensitive in the cracking model. As mentioned in Chapter 3, sensitivity analysis is a key step in local calibration. Five groups of sections, including No. 3, No. 115, No. 401, No.404 and No. 417 with 4, 6, 14, and 2 sections respectively, were used to perform the sensitivity analysis. The process was based on the comparison of the normalized sensitivity index (S_i^N) of each coefficient in the transfer function. The results of the sensitivity analysis are listed in Table 4-1.

Table 4-1 Sensitivity Analysis of Cracking Models

Model	Coefficients	HWY No3	HWY No115	HWY No401	HWY No417	HWY No404	Rank
		Normalized S_i^N	Normalized S_i^N	Normalized S_i^N	Normalized S_i^N	Normalized S_i^N	
Fatigue	C1	1.13	130	0.03	2.39	0.73	2
	C2	7.8	308	11.8	35.2	0.85	1
Cracking	C4	33	39	33	33	32	1
	C5	0	0	0	0	0	2

A statistical analysis of all sections used in this study was conducted to determine the range of the coefficients in the fatigue model. It was found in this model that C1 and C2 were in the range of 0.9 to 1.3 which was based on the performance of each road calculated separately. These results were reasonable under the conditions in Ontario. Comparatively, the default values of the global calibrated coefficients are 2 and 1.22 respectively.

After the scope of C1 and C2 is determined, a regression analysis was conducted by computing each section with the global calibrated model. The results showed a linear relationship between the coefficients C1, C2, and fatigue distress' common logarithm log (DI_F) in Table 4-2. Based on the collected data, the regression equation of each section shows a linear relationship in case of similar weather, material, structure, and traffic conditions. The following table lists the equations for each of the five groups of roads.

Table 4-2 Regression Equations of log(DI_F) and C1,C2

Item	Section	y1-log($DI_{Fbottom-up}$)	y2-log($DI_{Ftop-down}$)
N115	6	$y1 = 7.964 - 3.326 * C1 - 4.592 * C2$	$y2 = 11.351 - 4.111 * C1 - 6.736 * C2$
N401	14	$y1 = 10.362 - 4.283 * C1 - 7.317 * C2$	$y2 = 13.433 - 4.762 * C1 - 8.674 * C2$
N3	4	$y1 = 8.508 - 3.386 * C1 - 4.747 * C2$	$y2 = 11.609 - 4.212 * C1 - 7.058 * C2$
N404	4	$y1 = 10.087 - 4.269 * C1 - 8.538 * C2$	$y2 = 8.738 - 3.860 * C1 - 7.720 * C2$
N417	2	$y1 = 9.083 - 3.671 * C1 - 5.33 * C2$	$y2 = 13.35 - 5.41 * C1 - 13.349 * C2$

The principle of determination of C1 and C2 was to minimize the deviation of the fatigue damage values. Due to the allowable load repetitions obtained in Equation 4-1 unavailable in MEPDG output files, it is impossible to use non-linear method to optimize directly (Kaya et al. 2016). However, according to the regression equations above, an optimization could be employed to ensure the minimization of the deviation. By using LINGO software (LINDO System Inc.), the coefficients were optimized and C1 ,C2 is 1.1 and 1.0, respectively.

Based on the fatigue damage values recorded under the "Cracking Data" tab in the summary output in the MEPDG and the new values of C1 and C2 above, the coefficients C1 and C2 were determined by the non-linear method directly.

The step-by-step procedure of JPCP transverse cracking model local calibration is described as follows:

- Step 1: Based on the analysis of C1, C2, $DI_{bottom-up}$, and $DI_{top-down}$, the values of C1 and C2 are varied from 0.9 to 1.3. This makes the calculated $DI_{bottom-up}$ and $DI_{top-down}$ values change evenly among the testing sections. Optimal C1 and C2 were chosen based on

$DI_{bottom-up}$ and $DI_{top-down}$ values with minimal deviation from the five categories of sections in Table 4-2.

• Step 2: Both bottom-up and top-down fatigue damage were obtained by inputting the determined coefficients C1 and C2 into MEPDG. The values for each were extracted from the "Cracking Data" tab of the output files. MEPDG executes its calculations for the fatigue damage of each section to produce a calibration data set.

• Step 3: Through Equations 4-2 and 4-3, calibration coefficients C4 and C5 were optimized with the help of the nonlinear optimization approach (MS Excel Solver).

The results of the cracking sensitivity analysis from typical pavement section are presented below. Figure 4-1 compares the transverse cracking predictions using global models, and local calibration coefficients for calibration and validation sets. As can be seen in the figures, the transverse cracking model using global calibration coefficients could not accurately predict transverse-cracking distress in JPCP. This was obvious because there are no LTPP data for JPCP used for global calibration in Ontario. The difference between local conditions and policies may have led to the failure of prediction. Compared to using global calibration coefficients, the accuracy of the other model predictions was improved. As can be seen in Figure 4-2 and Figure 4-3, the predictive capacity of the cracking model improved significantly if the coefficients were calibrated locally, when compared with default values of the global calibration model.

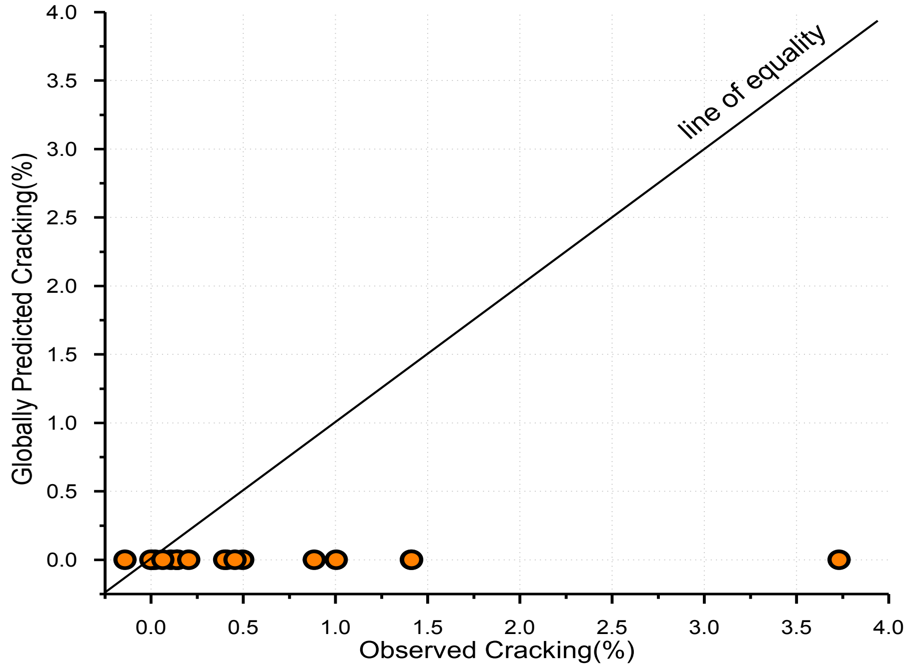

Figure 4-1 Transverse Cracking results with Global calibration

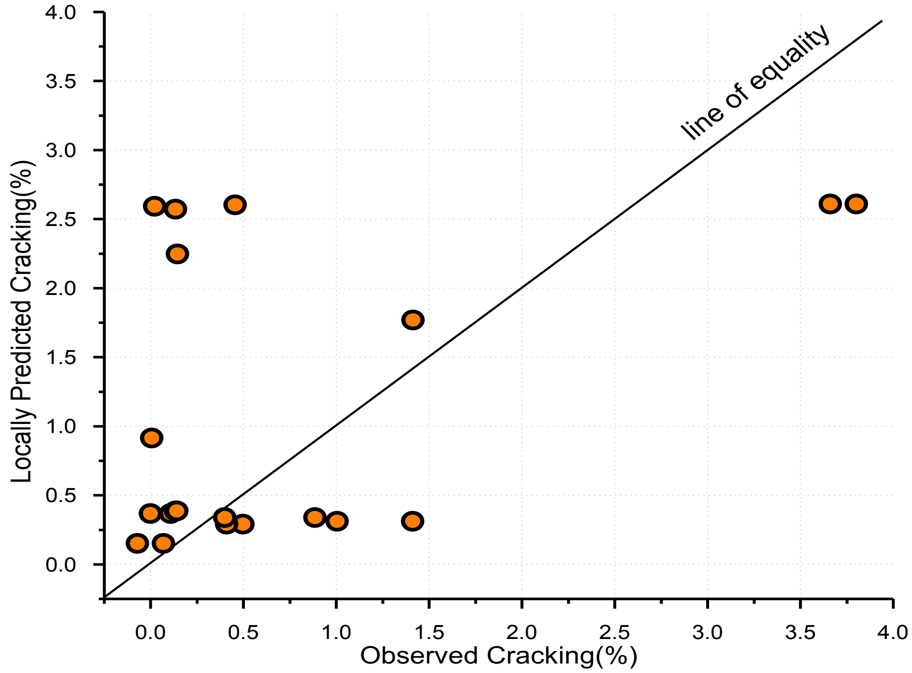

Figure 4-2 Transverse Cracking results with Calibration set

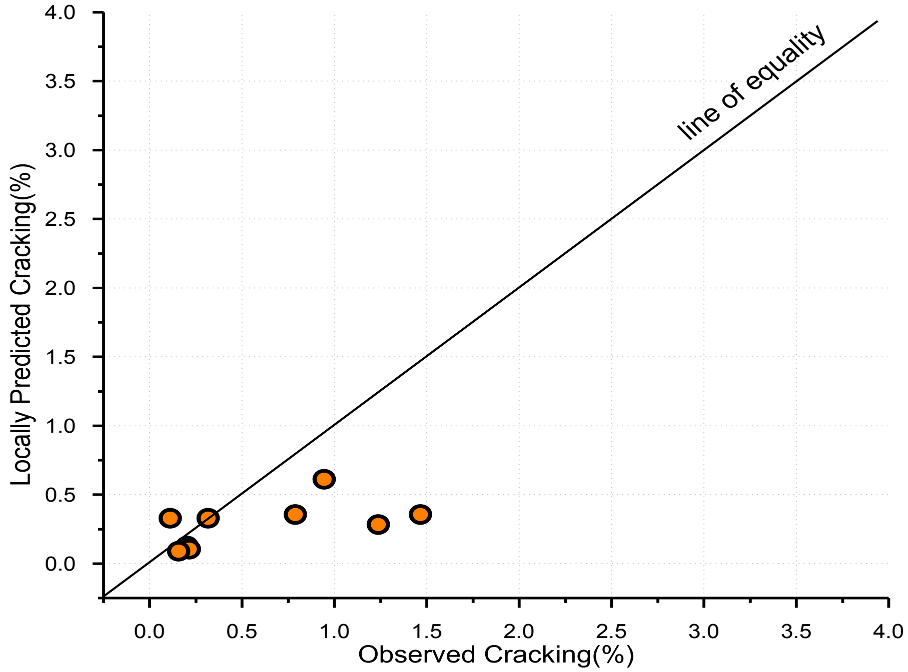

Figure 4-3 Transverse Cracking results with Validation set

Several indicators were used to evaluate the calibration results as described in Chapter 3. These include Average Bias (AB), Standard Error of Estimate (SEE), and Mean Absolute Percentage Error (MAPE). The results of comparison on local calibration can be seen in Table 4-3.

Table 4-3 Overall Precision Indicators of Cracking Calibration

Indicator	Global Calibration	Calibration Set(n=19)	Validate Set(n=9)
Average_Bias	-0.0057	-0.0042	-0.0031
Standard_Error	0.01	0.01	0.005
MAPE	1	3.6	0.64

On the other hand, a paired t-test was implemented with 95% certainty to assess the statistical significance of the MEPDG locally-calibrated predictions for selected sections. Table 4-4 shows that P= 0.175>0.05 and F =1.914< F-crit=3.996. This result shows that there is no significant difference between measured cracking and MEPDG predicted values and the results could be accepted.

Table 4-4 t-test Results For Transverse Cracking

Item (28)	Measured Cracking	Predicted Cracking
Mean	0.0057	0.01
Variation	7.9×10^{-5}	0.0001
P Value	0.175	
F Value	1.914	

4.3 Joint Faulting

The result of the sensitivity analysis was obtained based on the procedure described in Chapter 3, and sensitivity calculations of four typical roads are listed in Table 4-5.

Table 4-5 Faulting Sensitivity Analysis Results

Coefficients	No3	No115	No401	No417	Rank
	Normalized S_{ijk}^{N}	Normalized S_{ijk}^{N}	Normalized S_{ijk}^{N}	Normalized S_{ijk}^{N}	
C1	0.779	0.858	0.738	0.023	3
C2	1.304	1.5	1.327	0.037	2
C3	0.406	0.434	0.366	0.012	5
C4	0.541	0.577	0.539	0.02	4
C5	0	0	0.064	0	6
C6	5.231	6.815	5.134	0.18	1
C7	0	0	0.009	0	7

As shown in Table 4-5, C6 was the most sensitive coefficient in the transfer function, with the highest sensitivity index for each road section. C2 and C1 were the second and third most sensitive coefficient, followed by C3 and C4. It should be noted that C5 and C7 had the least effect on the prediction results and should not be calibrated with others.

For the transfer function of joint faulting, an incremental approach method was employed (AASHTO 2008). Based on this method, faulting values in one month are calculated cumulatively from the traffic opening date, to obtain the faulting value at any time.

Transverse joint faulting predictions can be determined from the following set of equations:

$$\mathrm{Fault}_m = \sum_{i=1}^{m} \Delta\mathrm{Fault}_i \tag{4-4}$$

$$\Delta\mathrm{Fault}_i = C_{34} \cdot (\mathrm{FaultMax}_{i-1} - \mathrm{Fault}_{i-1})^2 \cdot \mathrm{DE}_i \tag{4-5}$$

$$\mathrm{FaultMax}_i = \mathrm{FaultMax}_{i-1} + \left(\frac{C_7}{10^6}\right) \cdot \mathrm{DE}_i \cdot \log(1 + C_5 \cdot 5^{\mathrm{EROD}})^{C_6} \tag{4-6}$$

$$\mathrm{FaultMax}_0 = C_{12} \cdot \delta_{\mathrm{curing}}[\log(1 + C_5 \cdot 5^{\mathrm{EROD}}) \cdot \log\left(\frac{P_{200} \cdot \mathrm{WetDays}}{P_s}\right)]^{C_6} \tag{4-7}$$

Where:

Fault_m = Mean joint faulting at the end of month m, mm;

$\Delta\mathrm{Fault}_i$ = Incremental change (monthly) in mean transverse joint faulting during month i, mm;

$\mathrm{FaultMax}_i$ = Maximum mean transverse joint faulting for month i, mm;

$\mathrm{FaultMax}_0$ = Initial maximum mean transverse joint faulting, mm;

$EROD$ = Base/subbase erodibility factor;

DE_i = Differential density of energy of subgrade deformation accumulated during month I;

δ_{curing} = Maximum mean monthly slab corner upward deflection PCC due to temperature curling and moisture warping;

P_s = Overburden on subgrade, kg;

P_{200} = Percent subgrade material passing #200 sieve;

$WetDays$ = Average annual number of wet days with a rainfall of more than 2.54 mm;

$C_{1,2,3,4,5,6,7,12,34}$ = Calibration coefficients;

C_{12} and C_{45} are defined by the following equations:

$$C_{12} = C_1 + C_2 \times FR^{0.25} \tag{4-8}$$
$$C_{34} = C_3 + C_4 \times FR^{0.25} \tag{4-9}$$

Where:

FR = Base freezing index defined as the percentage of time the top base temperature is below freezing (0 ℃) temperature.

It should be noted that Equation 4-6 is a little different from the one presented in AASHTO Mechanistic-Empirical Pavement Design Guide, Interim Edition: A Manual of Practice (AASHTO 2008). The equation in the manual is:

$$\mathrm{FaultMax_i = FaultMax_{i-1}} + C_7 \cdot \mathrm{DE_i} \cdot \log(1 + C_5 \cdot 5^{\mathrm{EROD}})^{C_6} \quad (4\text{-}10)$$

According to the literature review the AASHTO Mechanistic-Empirical Pavement Design Guide, Interim Edition: A Manual of Practice (AASHTO 2008), Equation 4-10 cannot calculate the faulting properly. Based on communications with the developers of MEPDG (ARA 2014), it was noted that division of C_7 by 10^{6} in Equation 4-8 had been embedded in the software, although this division was not shown in the Equation 4-10 (Sachs 2015).

Components of each transfer function above can be inspected in output files of the software (Ceylan et al. 2009). Some information related to each variable is listed below, and have been confirmed by many examples (Sachs 2015).

- *Erodibility*, which is used as an input value, is known or can be checked from the "Design Properties" tab in the final result output file.
- *P200*, is an input value and is known or can be checked from the "Layer #" tab in the final result output file
- *Wet Days* can be found in the intermediate output file "MonthlyClimateSummary.csv" by summing all the wet days in all months, calculate the mean wet days in every month and then multiplying by 12 to obtain annual wet day results.
- *FAULTMAX 0* is provided in the first column and first row of the "JPCP_faulting.csv" as an intermediate file for each pavement section. Because the FAULTMAX0 value can be taken from the intermediate file, the curling and warping deflection value can be obtained using the FAULTMAX0 equation.
- *DE* can be extracted from the "Faulting Data" tab in the final result output file.
- *FR* is a key factor in calculating both coefficients C12 and C34, and calibrated results are much more sensitive to this parameter than others. This value can be found in an intermediate file named as 'GeneralInput.txt,'.
- *Ps* represents the overburden which can be determined using the following equation:

$$\mathrm{p_s} = 144 \cdot (\mathrm{Gam_{Pcc}} \cdot \mathrm{H_{Pcc}} + \mathrm{Gam_{base}} \cdot \mathrm{H_{base}}) \quad (4\text{-}11)$$

Where:

Gam_{PCC} = Unit weight of concrete (kg/cm^3);

Gam_{base} = Unit weight of base (kg/cm^3);

H_{Pcc} = Concrete thickness (cm.);

H_{base} = base thickness (cm.).

If the optimization procedure is based on MS-Excel worksheet, the step-by-step faulting calculation from available variables can be described as follows:

- Step 1: Before conducting faulting calculation, all the inputs should be identified either by checking the original output file or computing the values. These components include Wet-days, FAULTMAX0, FR, and DE, and can be found in corresponding files of outputs. However, Ps and Curling & warping deflection are calculated.
- Step 2: Use Equations 4-4 to 4-7 to calculate variables for each month.
- Step 3: Before calibration, make sure the faulting values calculated separately to match the values by MEPDG.
- Step 4: If the faulting value calculation is correct, the local calibration can be implemented using MS-Excel solver to optimize all the transfer function coefficients. The optimization includes minimizing the mean squared error (MSE) between the predicted values and the actual MTO PMS data regarding faulting measurements in the calibration data set. The set of local calibration coefficients is determined by the optimization procedure.
- Step 5: For validation purposes, the local calibration coefficient accuracy was evaluated using an independent validation data set.

Figure 4-4, Figure 4-5, and Figure 4-6 compare the faulting predictions using global and local calibration coefficients for calibration and validation datasets, respectively. The improvement on local calibration can be seen in Table 4-6.

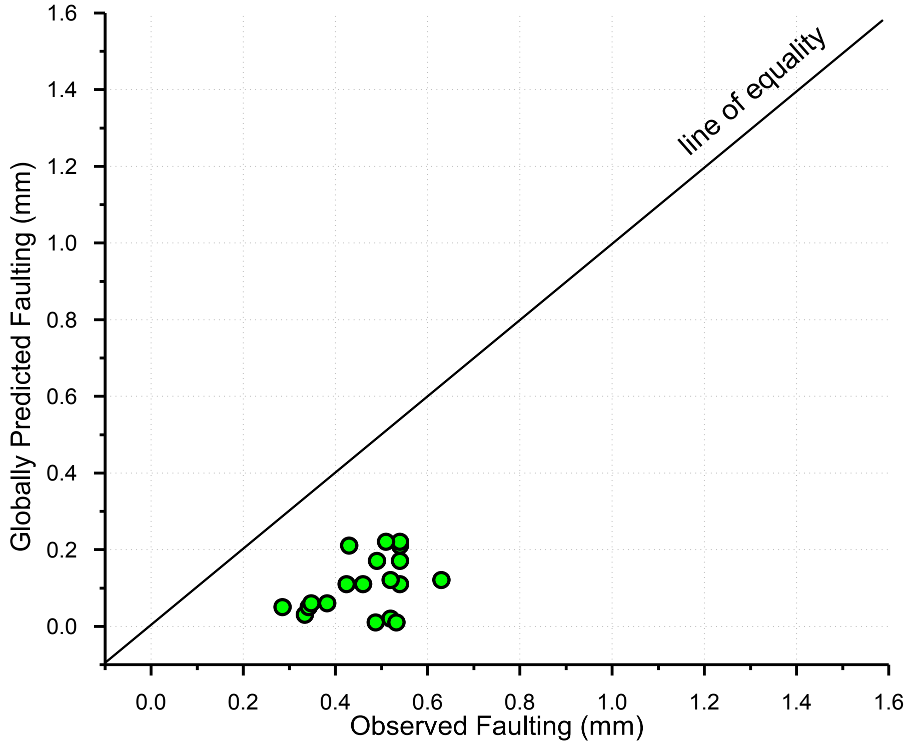

Figure 4-4 Faulting results with Global Calibration

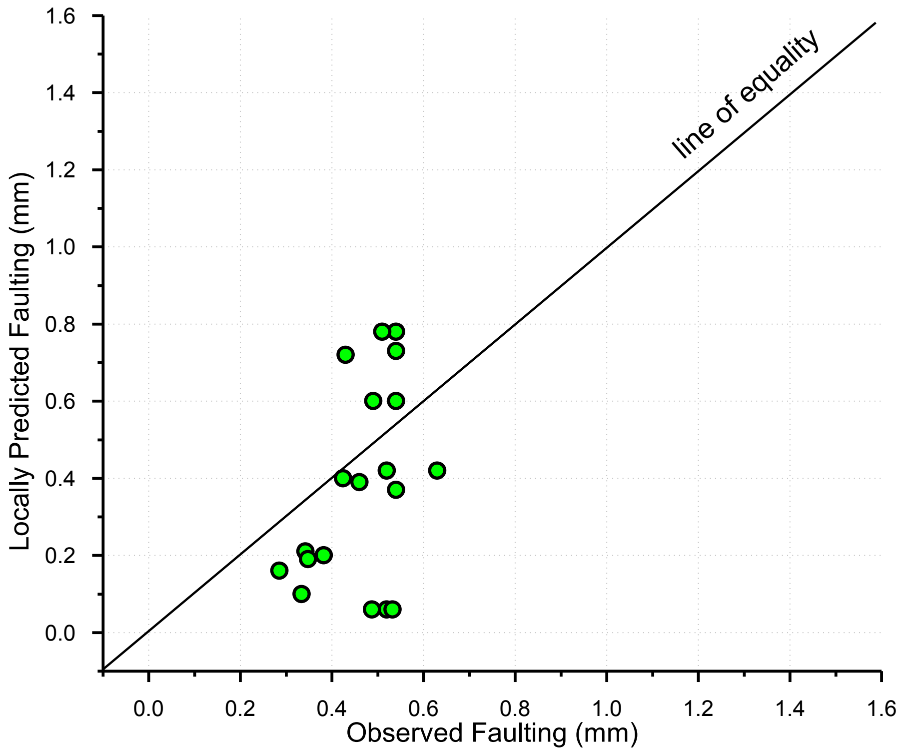

Figure 4-5 Faulting results with Calibration set

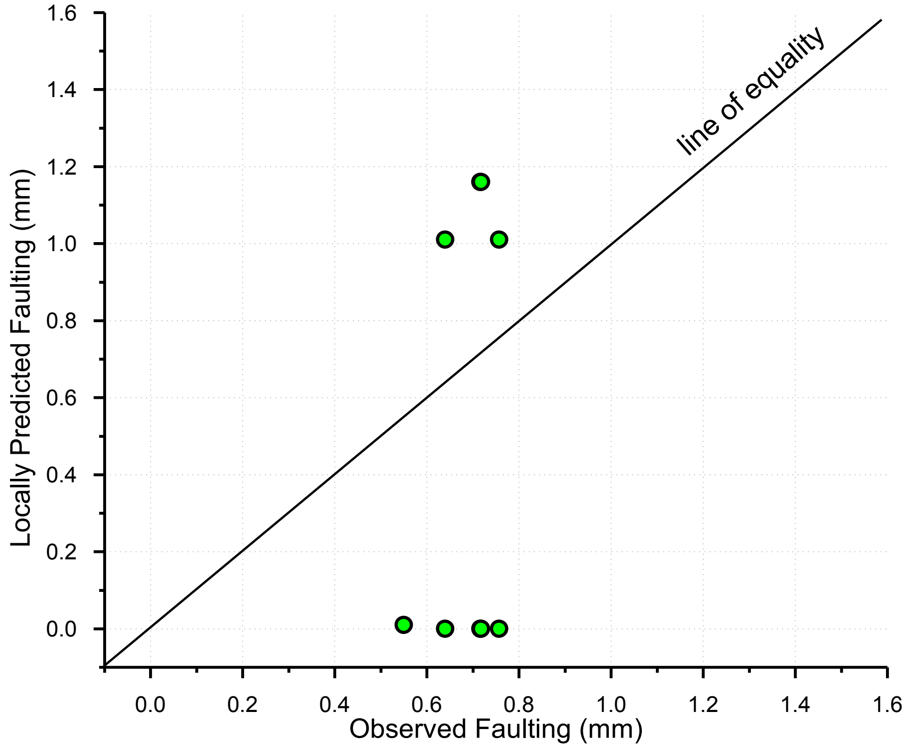

Figure 4-6 Faulting results with Validation set

Table 4-6 Overall Precision Indicators of Faulting Calibration

Item	Global Calibration	Calibration Set(n=19)	Validate Set(n=5)
Average_Bias	-0.357	-0.086	0.19
Standard_Error	0.368	0.243	0.42
MAPE	0.773	0.443	0.503

A paired t-test was implemented to assess the result of MEPDG locally-calibrated predictions for selected sections, and a p-value was calculated as 0.178>0.05, and F value was 1.88< F-crit=3.996. This result shows that, with 95 % certainty, there is no significant difference between measured faulting and MEPDG predicted faulting values (Table 4-7).

Table 4-7 T- test Results for Faulting Predictions

Item (24)	Measured Faulting	Predicted Faulting
Mean	0.466	0.38
Deviation	0.008	0.066
F Value	1.88	
P Value	0.178	

4.4 Smoothness (IRI)

The International Roughness Index (IRI) is the roughness index obtained from measured longitudinal road profiles. It is calculated using a quarter-car vehicle math model, whose response is accumulated to yield a roughness index with units of slope (in/mi, m/km, etc.). IRI is the road roughness index most commonly used worldwide for evaluating and managing road systems and the smoothness performance index used by the MEPDG. The MEPDG IRI prediction model for JPCP is a comprehensive indicator consisting of the transverse cracking prediction, the joint-faulting prediction, the spalling prediction, and a site factor, along with calibration coefficients. The JPCP IRI prediction equation employed in MEPDG is as follows:

$$\mathrm{IRI} = IRI_{ini} + C_1 \times \mathrm{CRK} + C_2 \times \mathrm{SPALL} + C_3 \times \mathrm{Fault} + C_4 \times \mathrm{SF} \qquad (4\text{-}12)$$

Where:

IRI = Predicted IRI, mm/km;

IRI_{ini} = Initial smoothness measured as IRI, mm/km;

CRK = Percent slabs with transverse cracks (all severities);

SPALL = Percentage of joints with spalling (medium and high severities);

Fault = Total cumulative joint faulting, cm;

SF = Site factor;

$C_{1,2,3,4}$ = Calibration coefficients.

The site factor of Equation 4-12 can be calculated as follows:

$$\mathrm{SF} = \mathrm{AGE} \cdot (1 + 0.5556 \times \mathrm{FI})(1 + \mathrm{P}_{200}) \times 10^{-6} \qquad (4\text{-}13)$$

Where:

AGE = Pavement Age, year;

FI = Freezing index, F-days;

P_{200} = Percent subgrade material is passing No. 200 sieve.

However, the JPCP IRI values reported in the MEPDG outputs could not be obtained using Equation 4-14, like equation 4-12. As Kaya pointed in his thesis, the corrected JPCP IRI equation should be used as follows:

$$\mathrm{IRI} = IRI_{ini} + C_1 \times \mathrm{CRK} + C_2 \times \mathrm{SPALL} + C_3 \times \mathrm{Fault} \times 5280/\mathrm{JSP} + C_4 \times \mathrm{SF} \qquad (4\text{-}14)$$

Where:

JSP = Joint spacing, m.

There are two potential methods to calibrate the IRI model using the cracking and faulting values, depending on whether they are global or local calibrated.

- Approach 1: Calibrate using locally-calibrated distress prediction models. It means that the models will use the locally calibrated transverse cracking and joint faulting results to predict IRI values.
- Approach 2: Calibrate only using globally-calibrated distress prediction models without considering the accuracy of the distress model in the local IRI model. Practitioners can determine whether the IRI model can be locally-calibrated with good accuracy without using the local calibration procedure of each of distress models. The local calibration of each model can be a time and cost consuming process.

The method for obtaining each variable required for IRI calculation was determined, and it was found that all the variables were either extracted from general or intermediate output files or calculated from data provided by the output files listed by following.

- IRIini: input in the software as an initial IRI value. It is also recorded in the final output file;
- CRK and Fault: can be obtained from the “Distress Data” tab in the final result summary output file;
- SPALL: can be obtained from an intermediate output file ‘Spalling.txt.';
- SF: can be calculated using Equation 4-13;
- FI for SF calculation can be obtained from the “Climate Inputs” tab in the final result output file;
- P 200 : a user-input value which is recorded in the “Layer #” tab in the final result summary output file.
- ‘JPCPIRIInput.txt’ is a file required for calculating IRI predicted value, as it contains various input parameters.

As can be seen in Equation 4-14, both transverse cracking and faulting predictions are involved in the calculation of IRI. In this study, local calibration of JPCP IRI model has referred to both locally and globally-calibrated transverse cracking and faulting values. The step-by-step procedure for local calibration of JPCP IRI model can be described as follows:

Step 1: IRI predictions for each year and each pavement section were calculated by inputting into Equation 4-13 and 4-14 all the relevant data collected from output files and intermediate files. For example, site factor values for each year were obtained using Equation 4-13. Locally-calibrated transverse cracking and faulting model predictions are used in Approach 1, while globally-calibrated transverse cracking and faulting model predictions are used as inputs to the IRI equation in Approach 2.

Step 2: The optimization procedure for local calibration coefficients was performed using a nonlinear optimization approach (MS Excel Solver) to minimize the Residual Sum Square (RSS) between predicted and actual IRI values. Coefficients were determined by minimizing the differences between IRI predictions and measurements.

Step 3: The set of calibration coefficients which result in the minimum RSS was then taken as the MEPDG local calibration coefficient set for the IRI model in either approach.

Figure 4-7, Figure 4-8, and Figure 4-9 compare the IRI predictions using global coefficients, and MEPDG local calibration coefficients for calibration and validation sets, respectively. As can be seen from the figures, the MEPDG locally-calibrated models produce more accurate predictions than the global model. Model accuracy was further improved by local calibration compared to that of the MEPDG globally calibrated model.

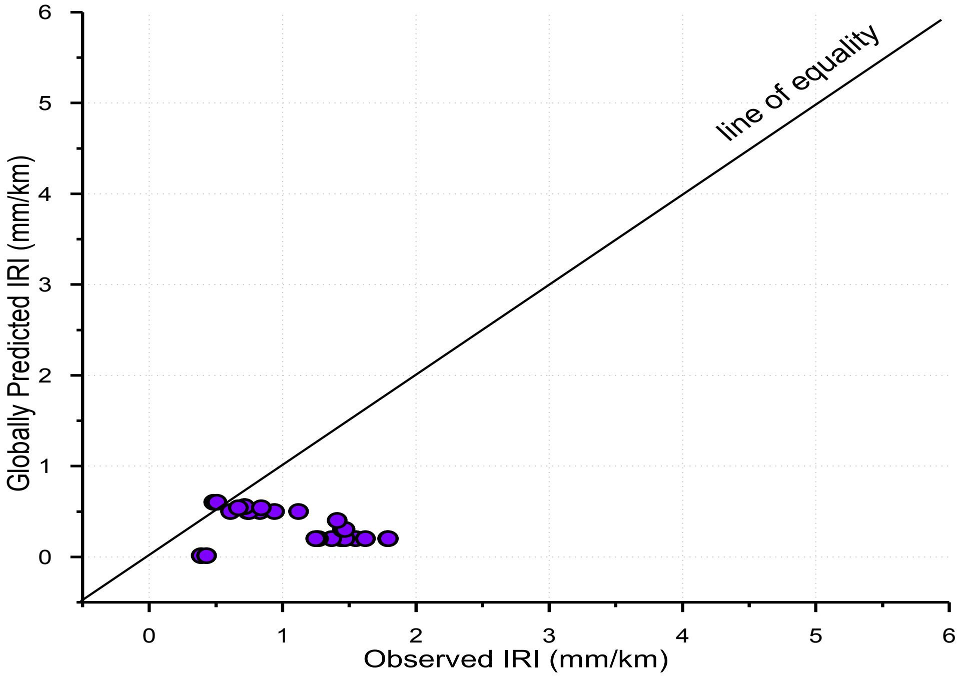

Figure 4-7 IRI results with global calibration

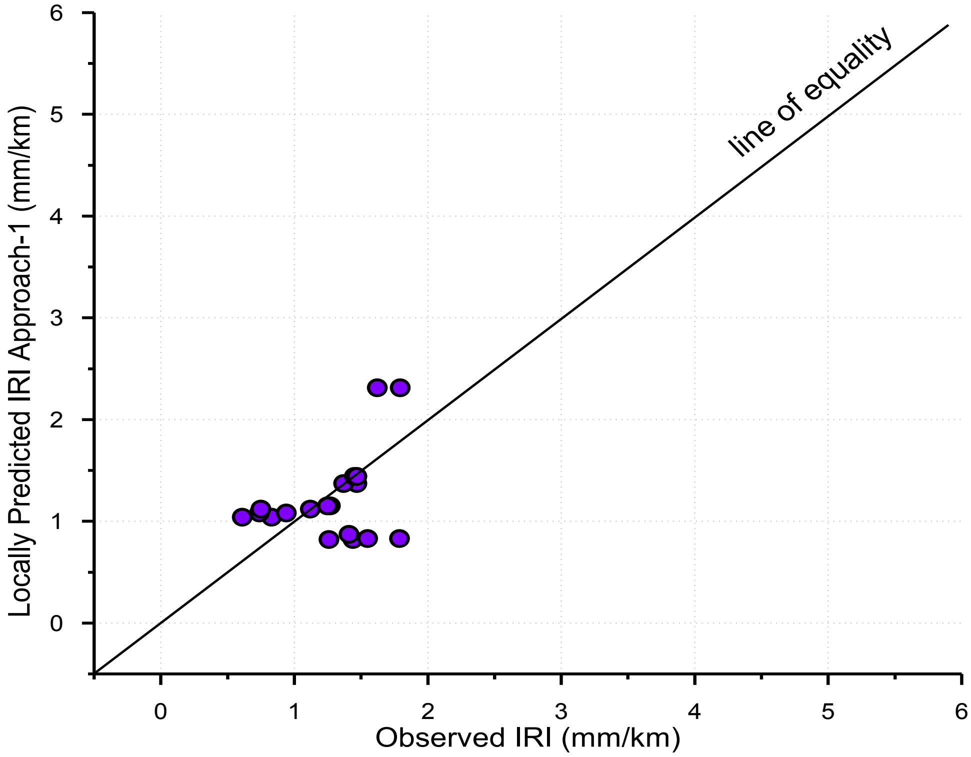

Figure 4-8 IRI results (App1) with local calibration set

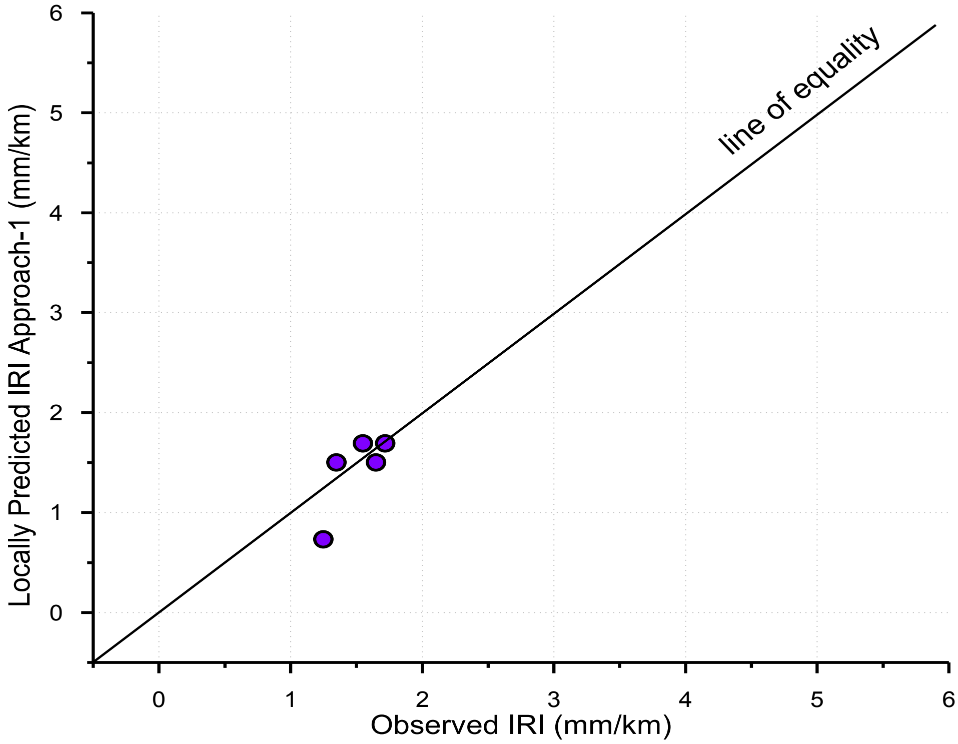

Figure 4-9 IRI results (App1) with local validation set

An auxiliary approach (Approach 2) was also developed to locally calibrate the IRI model using results of globally calibrated cracking and faulting predictions. As seen in Figure 4-10 and Figure 4-11, approach 2 can also improve IRI predictions to some extent. The purpose of using two approaches in the local calibration of IRI model is to determine if the model can be locally calibrated with sufficient accuracy without the local calibration procedure of each distress model. This could potentially save cost and data resources.

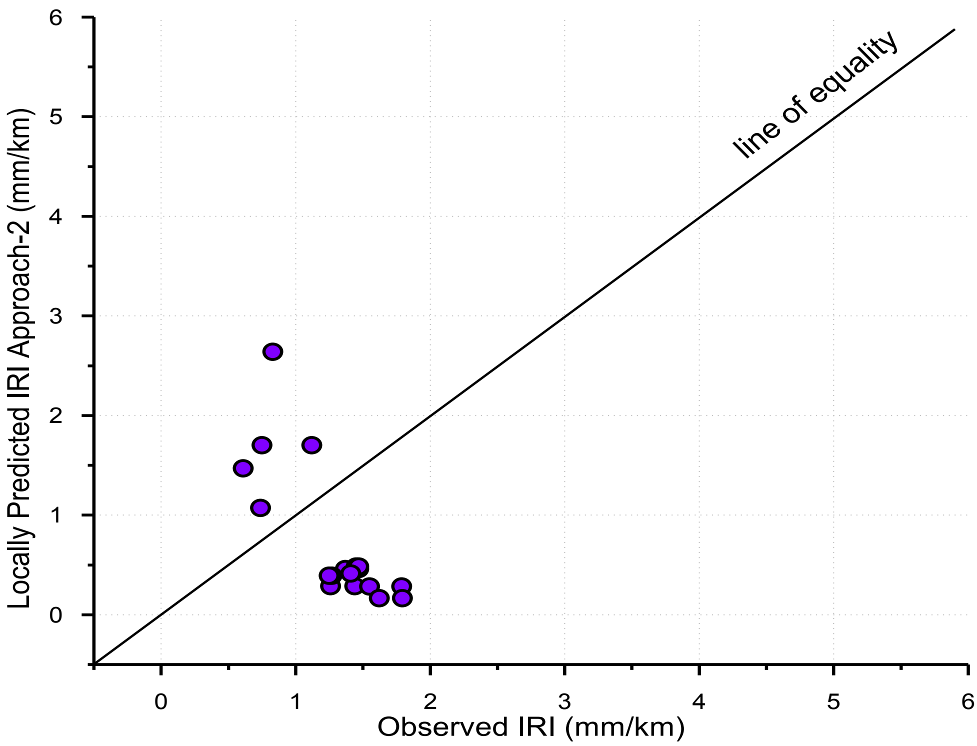

Figure 4-10 IRI results (App2) with local calibration set

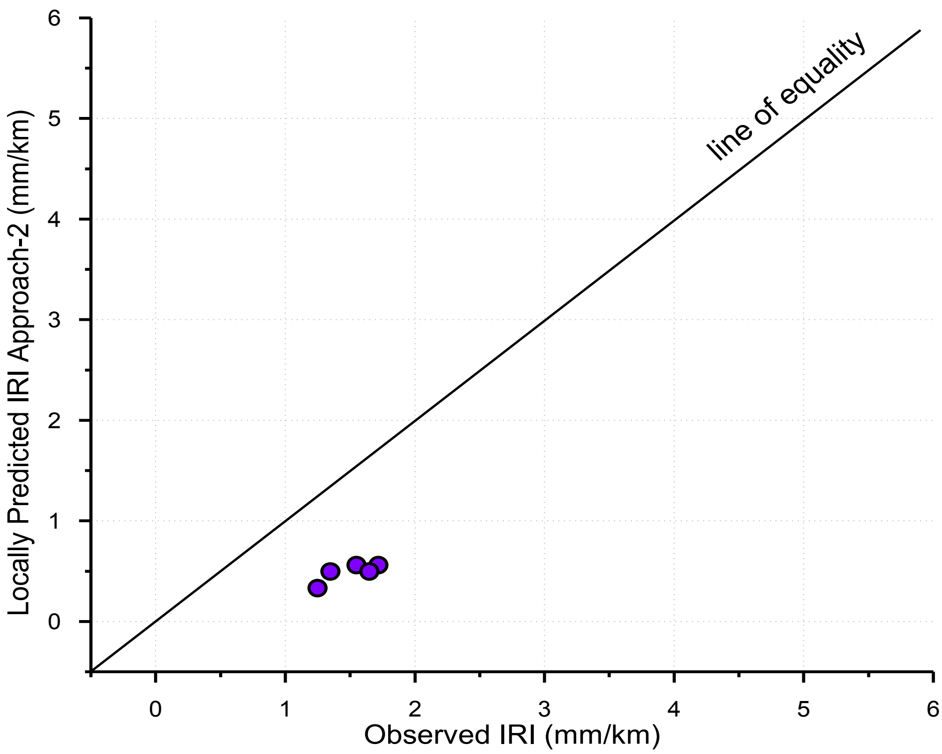

Figure 4-11 IRI results (App2) with local validation set

An implementation of Approach 1 would provide more accurate and precise results of local calibration; however, it would be difficult for those agencies who want to obtain IRI predictions as their assessment index without using locally-calibrated transverse cracking and faulting predictions. The improvement of Approach 1 on local calibration is clearly shown when compared with that of the global model, as seen in Table 4-8. In this study, it was clear that Approach 1 with a locally-calibrated IRI model can predict this indication with sufficient accuracy for Ontario JPCP pavement systems.

Table 4-8 Overall Precision Indicators of IRI Calibration

Item(24)	Global Calibration	Approach1		Approach2	
		Calibration Set(n=19)	Validate Set(n=5)	Calibration Set(n=19)	Validate Set(n=5)
Average_Bias	-0.05	-0.05	-1.01	-0.05	-1.01
Standard_Error	1.06	0.43	0.26	2.36	1.02
MAPE	0.69	0.27	0.14	1.33	0.67

A paired t-test was implemented to assess the result of MEPDG locally-calibrated predictions for selected sections. As for Approach 1, the p-value is 0.69 more than 0.05 and F value of 0.15 less than F-crit=3.996. This result shows that, with 95 % certainty, there is no significant difference between measured IRI and MEPDG predicted IRI.

Table 4-9 Pair test for JPCP IRI Predictions

Item(24)	Measured IRI	Predicted IRI	
		App1	App2
Mean	1.27	1.22	1.22
Variation	0.12	0.19	5.06
F Value		0.15	0.01
P Value		0.69	0.92

On the other hand, in Approach 2 the p-value was 0.92 more than 0.05 with F value of 0.01 less than F-crit=3.996. This result shows that, with 95 % certainty, there is no significant difference between measured IRI and locally predicted IRI, in Table 4-9. However, Approach 1 showed more accurate than Approach 2, as shown in Table 4-8.

4.5 Summary

Three distress models have been calibrated and validated with actual data from roads under the local conditions in Ontario. Among these models, the cracking model employed a method of trial-and-error, and optimization was used to find proper coefficients after data were processed and classified. The result of this calibration was a more accurate prediction of cracking as compared to a model using the global coefficients. The faulting and IRI models are calibrated using MS Excel® as an optimization method to identify the coefficients of transfer functions. For instance, faulting model calibration is developed by using MS Excel® Solver to do the optimization separate from the MEPDG software when all the components of the model are available. The results were evaluated by a series of indicators, including Standard Error Estimate (SEE), and T-test. By comparison, the local calibrated results were found to have higher accuracy and more efficient prediction than the globally calibrated coefficients.

Table 4-10 Local Calibration results of MEPDG

Distress Model	Coefficients	Global Calibration	Local calibration	
Faulting	C1	0.595	0.4	
	C2	1.638	1.116	
	C3	0.00217	0.00217	
	C4	0.00444	0.00444	
	C5	250	250	
	C6	0.47	0.9377	
	C7	7.3	7.3	
	C8	400	400	
Transverse Cracking	C1	2	1.1	
	C2	1.22	1.0	
	C4	0.52	102.4	
	C5	-2.17	-0.8277	
IRI			Approach1	Approach2
	C1	0.8203	0.8203	0.8203
	C2	0.4417	0.4417	0.4417
	C3	1.4929	16.145	6.17
	C4	25.24	56.944	25.24

However, these mathematical methods are not all-purpose, and sometimes they may lead to unreasonable solutions. For example, the solution could be too large or too small to meet the demands of a mathematical equation. Consequently, necessary constraints based on local engineering experience should be used to make these results to be in line with reality. In addition, the collection of more observed data would be helpful to achieve more precise results in the future. The results of local calibration in Ontario are shown in Table 4-10.

Chapter 5 Summary, Conclusions and Recommendations

5.1 Summary

In this research, the accuracy of a globally calibrated pavement performance prediction model was evaluated using MTO Pavement Management System data. For those global predictions which did not meet the requirements of the MTO, a local calibration was conducted to improve the prediction accuracy. This process was executed with the assistance of a series of mathematical techniques including sensitivity analysis, regression, and nonlinear optimization methods. The research was focused on doing the local calibration for concrete pavement (only JPCP) by using field measurements and forensic investigations.

Testing sections were selected from different regions of Ontario, with various traffic loads, age, and climatic conditions are taken into account, with a focus on pavements constructed after 1989. The MTO provided design information for pavement structure, traffic volume, and international roughness index (IRI). Meanwhile, weather and climate data were obtained from the weather stations near the selected sections.

In the local calibration of the MEPDG, two major steps were fulfilled, including (1) evaluation of the accuracy of the globally-calibrated MEPDG performance models and (2) calibration of these models when their accuracy was found to be too low. A series of techniques were applied to adjust the MEPDG distress models for rigid pavements under the local conditions in Ontario. Data were analyzed, and sensitivity analysis conducted to find the most important calibration coefficient for each transfer function. Subsequently, distress models were adjusted by changing the coefficients to calculate the prediction value that best correlated with the observed values for all sections.

Various optimization techniques in the local calibration process were used to improve the efficiency and accuracy of the prediction models, including transverse cracking, joint faulting, and IRI. The detailed information of components in transfer functions to perform local calibration was explored in intermediate and general output files, in which their locations are listed.

In order to find the relation between coefficients and fatigue damage, the OAT method was used. A series of regression equations were set up for different section groups based on the properties of traffic and structure of each section. Then, the Excel solver was applied to fit the proper coefficients in the transfer functions with comparisons to actual measurements from the MTO. Conclusions were drawn for rigid pavement, and corresponding coefficients of each performance model and recommendations for future improvement were also proposed.

5.2 Conclusions

In the case of the transverse cracking model, it was determined that C1 and C2 in fatigue models are related to the common logarithm of allowable traffic repetitions ($\log_{10} N_{Allowable}$). The relationship can be expressed as a linear regression equation which is depended on traffic, structure, and local conditions. Then, the appropriate coefficients were found due to the principle of making the fatigue damage deviation minimal.

All the values for factors were related to the weather, traffic loading, and other local conditions. The statistical data showed each coefficient in each function varied in a certain range. For example, C1 and C2 ranged from 0.9 to 1.3, C3 ranged from 2.3 to 3, and C4 varied from 0.6 to 3.7. Based on these constraints in the optimization process, the Excel non-linear method was employed to obtain the optimal solutions. The results showed there was a significant improvement in the local calibration in comparison with global coefficients.

The most sensitive factor in the joint faulting model was found to be C6, which showed a clear relation with moisture, pavement age, subgrade, and base type. This factor was followed by C2, C3, and C1, in terms of sensitivity, under the local conditions in Ontario. The statistical data also showed that these factors varied in a certain range. The range of each coefficient is shown in Table 5-1. Due to the availability of the components in the transfer function, the non-linear method was used to find the proper values of the coefficients. The results showed a significant improvement in accuracy of prediction was obtained.

As for the IRI model, an important difference seems to exist in initial IRI (IRI_0) after the pavements had been constructed when slip-form pavers came into use. Because of this application, better road quality was achieved, and IRI0 reduced about 30% compared with original construction methods. In this study, an incremental approach was used to employ a nonlinear model to predict IRI calibrated under the local conditions. As a result, IRI_0 was not taken into account during the survey. Site factors and joint faulting showed a higher impact on IRI than spalling and cracking. Consequently, the two corresponding coefficients (C1 and C2) for site and cracking were not changed in the transfer functions; however the other two coefficients were found by non-linear method. The results showed that the use of a calibrated model to predict IRI contributed to a higher accuracy in prediction than the global IRI model.

The recommended local calibration coefficients for use in design practice are summarized in Table 5-1. Each local calibration coefficient is listed along with the range of each coefficient.

Table 5-1 Results of Local Calibration

Item	Coefficients	Varying Range	Local Calibration	
Transverse-Cracking	C1	0.9~1.3	1.1	
	C2	0.9~1.3	1	
	C4	2.3~3	102.4	
	C5	0.6~3.7	-0.8277	
Joint faulting	C1	0.49~0.927	0.4	
	C2	1.15~3.169	1.116	
	C3	0.002~0.0029	0.00217	
	C4	0.0039~0.0063	0.00444	
	C5	250~263.6	250	
	C6	0.276~1.244	0.9377	
	C7	7.3	7.3	
	C8	400	400	
IRI			Approach 1	Approach 2
	C1	0.8203	0.8203	0.8203
	C2	0.4417	0.4417	0.4417
	C3	1.3~23	16.145	6.17
	C4	25~95	56.944	25.24

The findings in the study include the method of optimization, the local calibration strategy, and some mathematical optimization techniques that contribute to seeking the proper coefficients. The strategy of optimization requires that all the components in the transfer functions are known, and then the formed solution could be found separately using mathematical techniques. Thus, with the help of Excel solver and LINGO (LINDO System Inc.), the distress models can be calibrated outside the MEPDG software.

In the local calibration of the IRI model, two approaches were employed: (1) calibrate using only locally-calibrated distress prediction models which yield accurate results compared with performance measurements; (2) calibrate using globally-calibrated distress prediction models measurements, including transverse cracking and joint faulting, without considering agreement of performance model predictions observed performance. By comparison, Approach 1 is highly recommended due to its higher accuracy.

In conclusion, the research shows the feasibility of the mathematical optimization method for in local calibration in Ontario. Although it still needs improvements, the method could provide some useful findings for future uses of the MEPDG.

5.3 Recommendations

The MEPDG software is still developing, meaning that in every new version of the software some enhancements are added. Sometimes the models themselves are modified, as was the case with the ICM integrated climate module. The MEPDG would be much more conducive to local calibration if the following items could be considered in later versions:

- In the calibration, samples are usually divided into two parts, calibration and validation. Sometimes the effectiveness of validation is not consistent with that of calibration, and maybe poor or good due to the diversity of samples. Meanwhile, the selection of samples (testing roads) also influences the calibration results, which means different samples cause different coefficients and prediction errors. How to select these testing sections and achieve better results is an important topic in a future study, especially in the case of the limitation with the testing roads.
- For the convenience of local calibration, it is helpful to provide the reference information on the coefficient regression functions and correlative materials. Based on these materials, researchers can easily select a proper data set, find the scope of the coefficients, and obtain reasonable calibration results.
- Axle load spectrum is critical for the local calibration. In Ontario, this information can be downloaded from iCorridor, but the file cannot be recognized by the MEPDG (AASHTOWare Pavement 2.3.1). We strongly recommend that ARA eliminate the bugs to solve this compatibility problem.
- The data set selected to perform the calibration will affect the results of a calibration. In the process of choosing sections for calibration, a factorial design within these sections can ensure that the data set does not over-represent any particular design feature (e.g.

traffic or climate conditions). By increasing the number of available sections, a data set with reduced bias can be achieved by calibrating the models.

- An existing issue regarding the equations presented in the documentation in NCHRP Report 1-37A (2), concerns a crucial input to the faulting model needed to perform a calibration, the differential energy (DE). This value can be obtained from the "JPCP-faulting .csv" intermediate file for each month of the analysis and is used in the calculation of $Fmax_i$ as well as $\Delta Fault_i$. If the values in this file for differential energy (DE) are used in the faulting algorithm to calculate the faulting at each time increment, then the results are significantly larger than those from the model embedded in the MEPDG. As a result, the equation for $Fmax_i$ should be adjusted. In this study, the adjustment is to let correlative term multiply a constant (0.000001).
- In the calibration of the transverse cracking model, if the developer could provide more information on intermediate results of axle loading number in all cases and the allowable number of specified loading, it will be significantly helpful for the local calibration. The improvement would allow new versions of the software to be calibrated under local conditions quickly and easily. In addition, the relation between fatigue damage and load repetitions could be checked based on the traffic data in Ontario.
- From the conclusions in this study, we can see that the optimization method is not all-purpose. In order to obtain reasonable solutions, necessary constraints or boundaries on the coefficients are needed based on local engineering experience in order to make the study more in line with reality. In addition, more observed data in field work would be helpful to achieve more precise results.

Finally, the local calibration for rigid pavement in Ontario is a good experience in finding a proper way to implement the MEPDG for MTO, and hopefully, it can streamline the local calibration for other agencies in the future.

REFERENCES

AASHTO. (1993) Guide for design of pavement structures, Washington D.C.: American Association of State Highway and Transportation Officials.

AASHTO. (2008). Mechanistic-Empirical Pavement Design Guide-A Manual of Practice. American Association of State Highway and Transportation Officials, Washington, D.C.

AASHTO. (2010). Guide for the Local Calibration of the Mechanistic-Empirical Pavement Design Guide, American Association of State Highway and Transportation Officials, Washington, D.C.

AASHTO. (2011). Software Help System DARWin-ME Mechanistic-Empirical Pavement Design Software, American Association of State Highway and Transportation Officials, Washington, D.C.

AASHTO. (2013). AASHTOWare Pavement ME Design User™ Manual, American Association of State Highway and Transportation Officials, Washington, D.C.

Ahmed, S. E., Yuan, X. X., Lee, W., Li, N. (2016). Local Calibration of Cracking Models in MEPDG for Ontario's Flexible Pavement. TAC 2016: Efficient Transportation-Managing the Demand-2016 Conference and Exhibition of the Transportation Association of Canada.

ARA Inc. (2004). Guide for mechanistic-empirical design of new and rehabilitated pavement structures, Champaign.

ARA, Inc. (2013). AASHTOWare Pavement ME Design Software Version 2.1. www.me-design.com/MEDesign/Software.aspx. Accessed July 15, 2015.

Arellano, A., de Farias, M.M., de Souza, R.O., Ganesan, V.P.K., McDonald, M.P., Morian, D., Neto, S.D., Smith, J.T., Stoffels, S.M., Tighe. S.L., (2004). Improving Pavements with Long-Term Pavement Performance: Products for Today and Tomorrow. *The 2003–2004 International Contest on Long-Term Pavement Performance Data Analysis.* American Society of Civil Engineers (ASCE). Transportation and Development Institute (T&DI), Federal Highway Administration Long-Term Pavement.

Ayed, A., Tighe, S.L. (2015). Local Calibration for Mechanistic-Empirical Design using Genetic Algorithm. Transportation Association of Canada.

Barati, R. (2013). Application of excel solver for parameter estimation of the nonlinear Muskingum models. KSCE Journal of Civil Engineering, 17(5), 1139-1148.

Baus, R. L., Stires, N. R. (2010). Mechanistic-empirical pavement design guide implementation (No. FHWA-SC-10-01).

Bautista, F. E., Basheer, I., (2008.9). Jointed Plain Concrete Pavement (JPCP) Preservation and Rehabilitation Design Guide. Office of Pavement Design Pavement Design & Analysis Branch. California Department of Transportation of Design.

Brink, W. C. (2015). Use of statistical resampling techniques for the local calibration of the pavement performance prediction models. Michigan State University.

Bustos,M., Cordo, O., Girardi, P., Pereyra, M.(2012). Calibration of Distress Models from the Mechanistic–Empirical Pavement Design Guide for Rigid Pavement Design in Argentina. Journal of the Transportation Research Board. Washington. Transportation Research Board of the National Academies. DOI: 10.3141/2226-01

Ceylan, H., Coree, B., Gopalakrishnan, K.,(2009). Evaluation of the mechanistic-empirical pavement Design Guide for Implementation in Iowa. Iowa State University.

Ceylan, H., Gopalakrishnan, K., (2007). Neural Networks Based Models for Mechanistic-Empirical Design of Rubblized Concrete Pavements. Denver, CO. New Peaks in Geotechnics.

Ceylan, H., S. Kim, K. Gopalakrishnan, and D. Ma. (2013). Iowa Calibration of MEPDG Performance Prediction Models. Iowa: Institute for Transportation, Iowa State University.

Ceylan, H., Schwartz, C.W., Kim, S., and Gopalakrishnan, K., (2009). Accuracy of predictive models for dynamic modulus of hot mix asphalt. Journal of Materials in Civil Engineering, ASCE, Vol. 21, No. 6, June, pp. 286-293.

Darter, M. I., L. T. Glover, and H. L. Von Quintus. (2009). Implementation of the Mechanistic-Empirical Pavement Design Guide in Utah: Validation, Calibration, and Development of the UDOT MEPDG User's Guide. Report no. UT-09.11, IL: ARA, Inc.

Darter, M. I., Titus-Glover, L., Von Quintus, H., Bhattacharya, B. B., & Mallela, J. (2014). Calibration and Implementation of the AASHTO Mechanistic‐Empirical Pavement Design Guide in Arizona (No. FHWA-AZ-14-606).

Fernando, E.G, Oh, J., Ryu, D., Phase 1 of MEPDG program Implementation in Florida. Texas Transportation Institute Report D04491/PR15281-1. College Station TX, 2008.

FHWA. (2010a). “Local calibration of the MEPDG using pavement management.” Final Rep. for FHWA Project DTFH61-07-R-00143, Vol. I, Washington, DC.

FHWA. (2010b). “Local calibration of the MEPDG using pavement management.” Final Rep. for FHWA Project DTFH61-07-R-00143, Vol. II, Washington, DC.

Frontline Systems, Inc. (2017). Excel Solver - GRG Nonlinear Solving Method Stopping Conditions www.solver.com/excel-solver-grg-nonlinear-solving-method-stopping-conditions. Accessed June 22, 2017.Frontline Solvers®, www.solver.com

Gautam, G. P., Yuan, X. X., Lee, W., Li, N. (2016). Local Calibration of the MEPDG Rutting Models for Ontario's Flexible Roads: Recent Findings. Transportation Research Board 95th Annual Meeting (No. 16-3824).

Gulfam, E. Jannat, Tighe, S. L. (2016). An experimental design-based evaluation of sensitivities of MEPDG prediction: investigating main and interaction effects. International Journal of Pavement Engineering, 17(7), 615-625.

Gulfam, E. Jannat,. (2017). Developing Cost-Effective Pavement Maintenance and Rehabilitation Schedules: Application of MEPDG-Based Distress Models and Key Performance Index.

Hamdi, A. (2015). Local Calibration of AASHTOWare® Using Ontario Pavement Management System Data PMS2.

Holt, A., Sullivan, S., Hein, D. (2011). Life cycle cost analysis of municipal pavements in southern and eastern Ontario. In 2011 Conference and Exhibition of the Transportation Association of Canada.

Hsie, M., Ho, Y. F., Lin, C. T., Yeh, I. C. (2012). Modeling asphalt pavement overlay transverse cracks using the genetic operation tree and Levenberg–Marquardt Method. Expert Systems with Applications, 39(5), 4874-4881.

Huang, Y.H., (2003). Pavement Analysis and Design (2nd Edition), Pearson Education Inc., USA.

Hudson, W. R., Visser, W., Dougan, C., Monismith, C.L., (2011). Using State PMS Data to Validate the New Mechanistic/Empirical Pavement Design Guide (MEPDG). In 7th International Conference on Managing Pavement Assets.

Kaya O,(2015).Investigation of AASHTOWare Pavement ME Design/Darwin-ME Performance Prediction Models for Iowa Pavement Analysis and Design. Iowa State University.

Kaya, O., Kim, S., Ceylan, H., and Gopalakrishnan, K. (2016). Optimization of Local Calibration Coefficients of AASHTOWare Pavement ME Design Jointed Plain Concrete Pavement Performance Models. In Transportation Research Board 95th Annual Meeting (No. 16-4138).

Kim, S., Ceylan, H., Ma, D., and Gopalakrishnan, K. (2014). Calibration of pavement ME design and mechanistic-empirical pavement design guide performance prediction models for Iowa pavement systems. Journal of Transportation Engineering, 140(10), 04014052.

Kim, S., H. Ceylan, K. Gopalakrishnan, and O. Smadi. (2010). Use of pavement management information system for verification of Mechanistic-Empirical Pavement Design Guide performance predictions. Transportation Research Record 2153: 30-39. Washington DC:Transportation Research Board, National Research Council.

Levenberg, K. (1944). A method for the solution of certain non-linear problems in least squares. Quarterly of applied mathematics, 2(2), 164-168.

Li, Q.,Xiao, D., Wang, K.C. P., Hall, K. & Qiu, Y. (2011). Mechanistic-empirical pavement design guide (MEPDG): a bird's eye view. Journal of Modern Transportation. Volume 19, January 2011, P114-133, DOI:10.1007/BF03325749.

Mallela, J., Titus-Glover, L., Bhattacharya, B. B., Gotlif, A., and Darter, M. I. (2015). Recalibration of the JPCP Cracking and joint faulting Models in the AASHTO ME Design Procedure. In Transportation Research Board 94th Annual Meeting (No. 15-5222).

Mallela, J., Titus-Glover, L., Sadasivam, S., Bhattacharya, B., Darter, M., & Von Quintus, H. (2013). Implementation of the AASHTO Mechanistic-empirical pavement design guide for Colorado (No. CDOT-2013-4).

Mallela, J., Titus-Glover, L., Von Quintus, H., Darter, M. I., Stanley, M., and Rao, C. (2009). Implementing the AASHTO Mechanistic-Empirical Pavement Design Guide in Missouri Volume II: MEPDG Model Validation and Calibration. Missouri Department of Transportation.

Marquardt, D. W. (1963). An algorithm for least-squares estimation of nonlinear parameters. Journal of the society for Industrial and Applied Mathematics, 11(2), 431-441.

MTO. (1998). Construction Specification for Concrete Pavement and Concrete Base. Toronto: Ministry of Transportation, Ontario.

MTO. (2010). Highway Infrastructure Innovation Funding Program (HIIFP) Topic 6: Database for the Calibration of Mechanistic-Empirical Pavement Design Guide (M-E PDG) Distress Models.

MTO. (2013). Highway Infrastructure Innovation Funding Program (HIIFP) Topic 6: Local Calibration of Mechanistic-Empirical Pavement Design Guide (MEPDG) Distress Models for Ontario Conditions.

MTO. (2014). Ontario's Default Parameters for AASHTOWare Pavement ME Design Interim Report – 2014. Toronto: Ministry of Transportation, Ontario.

MTO. (2015). Highway Infrastructure Innovation Funding Program (HIIFP) Topic 6: Local Calibration of the Mechanistic-Empirical Pavement Design Guide (MEPDG) Prediction Models Using More Accurate

Field Measurements

NCHRP. (2004). Guide for Mechanistic-Empirical Design of New and Rehabilitated Pavement Structures. National Cooperative Highway Research Program 1-37A. Washington, DC: Transportation Research Board, National Research Council.

NCHRP. (2005). Traffic Data Collection, Analysis, and Forecasting for Mechanistic Pavement Design. National Cooperative Highway Research Program 01-39. Washington, DC: Transportation Research Board, National Research Council.

NCHRP. (2006a). Independent Review of the Mechanistic-Empirical Pavement Design Guide and Software. Research Results Digest 307. National Cooperative Highway Research Program 1-40 A. Washington, DC: Transportation Research Board, National Research Council.

NCHRP. (2006b). Changes to The Mechanistic-Empirical Pavement Design Guide Software Through Version 0.900-July, 2006. Research Results Digest 308. National Cooperative Highway Research Program 1-40 D. Washington, DC: Transportation Research Board, National Research Council.

NCHRP. (2009). Local Calibration Guidance for the Recommended Guide for Mechanistic-Empirical Pavement Design of New and Rehabilitated Pavement Structures. National Cooperative Highway Research Program Project 1- 40B Report, Washington, DC: Transportation Research Board of the National Academies.

NCHRP. (2010). Models for Predicting Reflection Cracking of Hot-Mix Asphalt Overlays. National Cooperative Highway Research Program Project 01-41 Report, Washington, DC: Transportation Research Board, National Research Council.

NCHRP. (2011). Sensitivity Evaluation of MEPDG Performance Prediction. National Cooperative Highway Research Program Project 01-47 Report, Washington, DC: Transportation Research Board, National Research Council.

NCHRP. (2013). Guide for Conducting Forensic Investigations of Highway Pavements. National Cooperative Highway Research Program Project 01-49 Report, Washington, DC: Transportation Research Board, National Research Council.

NCHRP. (2014). Implementation of the AASHTO Mechanistic-Empirical Pavement Design Guide and Software: A Synthesis of Highway Practice. National Cooperative Highway Research Program Project 20-05 Report, Washington, DC: Transportation Research Board, National Research Council.

NCHRP. (2015). Consideration of Preservation in Pavement Design and Analysis Procedures. National

Cooperative Highway Research Program Project 01-48 Report, Washington, DC: Transportation Research Board, National Research Council.

Rahman, M., Murshed, N. (2014). Sensitivity of Rigid Pavement Responses to Pavement Layer Thickness Due to Wheel Load: A Nonlinear Finite Element Study. Bangladesh: Trends in Transport Engineering and Applications, Volume 1, Issue 1.

Sachs, S., Vandenbossche, J. M., Snyder, M. B. (2015). Calibration of National Rigid Pavement Performance Models for the Pavement Mechanistic–Empirical Design Guide. Transportation Research Record: Journal of the Transportation Research Board, (2524), 59-67.

Schram, S., and M. Abdelrahman. (2006). Improving prediction accuracy in mechanistic-empirical pavement design guide. Transportation Research Record 1947: 59-68. Washington DC: Transportation Research Board, National Research Council.

Schwartz, C. W., Kim, S. H., Cylan, H.,(2011). Sensitivity Evaluation of MEPDG Performance Prediction, Final Report. National Cooperative Highway Research Program Transportation Research Board of the National Academies.

TAC, 2013. Pavement Asset Design and Management Guide (PADMG). Ottawa: Transportation Association of Canada.

Tia, M., Verdugo, D., Kwon, O. (2012). Evaluation of Long-Life Concrete Pavement Practices for Use in Florida (No. UF Project no. 00093785). Department of Civil and Coastal Engineering University of Florida.

Titus-Glover, L. and J. Mallela. (2009). Guidelines for Implementing NCHRP 1-37A M-E Design Procedures in Ohio Volume 4 - MEPDG Models Validation & Recalibration. Applied Research Associates, Inc.

Tompkins, D., Johanneck, L., and Khazanovich, L. (2015). State Design Procedure for Rigid Pavements Based on the AASHTO Mechanistic–Empirical Pavement Design Guide. Transportation Research Record: Journal of the Transportation Research Board, (2524), 23-32.

Velasquez, R., K. Hoegh, l. Yut, N. Funk, G. Cochran, M. Marasteanu, and L. Khazanovich. (2009). Implementation of the MEPDG for New and Rehabilitated Pavement Structures for Design of Concrete and Asphalt Pavements in Minnesota. MN/RC 2009-06, Minneapolis, Minnesota: University of Minnesota.

VonQuintus, H. L., Mallela, J., Bonaquist, R., Schwartz, C. W., and Carvalho, R. L. (2012). "NCHRP

REPORT 719 Calibration of Rutting Models for Structural and Mix Design." T.R. BOARD, ed., American Association of State Highway and Transportation Washington, D.C.

Wassem,A. (2013). Methodology Development and Local Calibration of MEPDG Permanent Deformation Models for Ontario's Flexible Pavements. Ryerson University.